REFERENCES

Bhatia, A., Y., Rahul, K.G., Bhattacharya, S.N., and Choi, H.J. (2007) Compatibility of Biodegradable Poly(lactic acid) (PLA) and Poly(butylene succinate) (PBS) Blends for Packaging Application. Korea-Australia Rheology Journal, 19, 125-131.

Becquart, F., Taha, M., Zerroukhi, A., Kaczun, J., and Llauro, M.F. (2007) Microstructure and properties of poly(vinyl alcohol-co-vinyl acetate)-g-ε-caprolactone. European Polymer Journal, 43, 1549-1556.

Burt, H.M., Jackson, J.K., Bains, S.K., Liggins, R.T., Oktaba, A.M.C., Arsenault, A.L., and Hunter, W.L. (1995) Cancer Letters, 88, 73-79.

Brown, S.B. (1991) Annual Reviews of Material Science, 21, 409-435.

Brown, M.W.R., Johnson, A.F., and Coates, P.D. Reactive Processing of Polymers. United Kingdom: Rapra Technology Limited.

Cabedo, L., Giménez, E., Lagaron, J.M., Gavara, R., and Saura, J.J. (2004) Development of EVOH-kaolinite nanocomposites. Polymer, 45, 5233-5238.

Caneba, G.T. (2005) Encyclopedia of Chemical Processing. Michigan: Taylor & Francis Group.

Cerrada, M.L., Pérez, E., Pereña, J.M., and Benavente, R. (1998) Wide-angle X-ray diffraction study of the phase behavior of vinyl alcohol-ethylene copolymers. Macromolecules, 31, 2559-2564.

Chaudhary D.S., Prasad, R., Gupta, R.K., and Bhattacharya, S.N. (2005) Clay intercalation and influence on crystallinity of EVA-based clay nanocomposites. Thermochimica Acta, 433, 187-195.

Chen, L., Qiu, X., Deng, M., Hong, Z., Luo, R., Chen, X., and Jing, X. (2005) The starch grafted poly(L-lactide) and the physical properties of its blending composites. Polymer, 46, 5723-5729.

Coates, J. (2000) Interpretation of Infrared Spectra, A Practical Approach. Chichester: John Wiley & Sons Ltd.

Cui, L., Ma, X., and Paul, D.R. (2007) Morphology and properties of nanocomposites formed from ethylene-vinyl acetate copolymers and organoclays. Polymer, 48, 6325-6399.

Fernández, M.D., and Fernández, M.J. (2008) Thermal decomposition of copolymers from ethylene with some vinyl derivatives. Journal of Thermal Analysis and Calorimetry, 91(2), 447-454.

Finkenstadt, V.L., and Willet, J.L. (2005) Reactive Extrusion of Starch-Polyacrylamide Graft Copolymers: Effects of Monomer/Starch Ratio and Moisture Content. Macromolecular Chemistry and Physics, 206, 1648-1652.

Hanley, S.J., Nesheiwat, A.M., Chen, R.T, Jamieson, M., Pearson, R.A., Sperling, L.H. (2000) Phase Separation in Semicrystalline Blends of Poly(phenylene sulfide) and Poly(ethylene terephthalate). II. Effect of Poly(phenylene sulfide) Homopolymer Solubilization of PPS-graft-PET Copolymer on Morphology and Crystallization Behavior. Journal of Polymer Science, 38, 4, 599-610.

Hasook, A., Muramaysu, H., Tanoue, S., Iemoto, Y., and Unryu, T. Effect of screw rotating speed on the properties of poly lactic acid(PLA)/organoclay nanocomposites prepared by twin-screw extruder.

Hyon, S.H., Jamshidi, K., and Ikada, Y. (1997) Synthesis of polylactides with different molecular weights. Biomaterials, 18, 1503-1508.

Ikada, Y., and Tsuji, H. (2000) Biodegradable Polyesters for Medical and Ecological Applications. Macromolecular Rapid Communications, 21, 117-132.

Jacobsen, S., Fritz, H.G., Ph. Degée., Ph. Dubois., and Jérôme, R. (2000) Single-step reactive extrusion of PLLA in a corotating twin-screw extruder promoted by 2-ethylhexanoic acid tin(II) salt and triphenylphosphine. Polymer, 41, 3395-3403.

Janata, M., Masař, B., Toman, L., Vlček, P., Brus, J., and Holler, P. (2003) Synthesis of novel type of graft copolymers by a “grafting-from” method using ring-opening polymerization of lactones and lactides. Reactive and Functional Polymers, 57, 137-146.

Janssen, L.P.B.M. (2004) Reactive Extrusion Systems. New York: Marcel Dekker.

Jiang, H., He, J., Liu, J., and Yang, Y. (2002) Synthesis and characterization of poly(ethylene-co-vinyl alcohol)-graft-poly(epsilon-caprolactone). Polymer Journal, 34, 682-686.

Kim, P.J., and White, J.L. (1994) Transesterification of ethylene vinyl acetate copolymer in a modular intermeshing twin screw extruder with different screw configurations. Journal of Applied Polymer Science, 54, 33-45.

Lambla, M., Druz, J., Bouilloux, A. (2004) Transesterification reactions in molten polymers. Polymer Engineering and Science, 27(16), 1221-1228.

Lewitus, D., McCarthy, S., Ophir, A., and Kenig, S. (2006) The effect of nanoclays on the properties of PLLA-modified polymers part 1: mechanical and thermal properties. Journal of Polymer Environment, 14, 171-177.

Lui, Y., Tian, F., and Hu, K.A. (2004) Synthesis and characterization of brush-like copolymer of polylactide grafted onto chitosan. Carbohydrate research, 339, 845-851.

Moraes, M. A. R., Moreira, A. C. F., Barbosa, R. V., and Soares, B. G. (1996) Graft Copolymer from Modified Ethylene-Vinyl Acetate (EVA) Copolymers. 3. Poly(EVA-*g*-Methyl Methacrylate) from Mercapto-Modified EVA. Macromolecules, 29, 416-422.

Ogata, N., Jimenez, G., Kawai, H., and Ogihara, T.J. (1997) Structure and thermal/mechanical properties of poly (l-lactide)-clay blend, Journal of Polymer Science part B: Polymer Physics, 35 , 389- 396.

Qi, F., and Hanna, M.A. (1999) Rheological Properties of Amorphous and Semicrystalline Polylactic Acid Polymers. Industrials Crops and Products, 10 , 47-53.

Ray, S.S., and Bousmina, M. (2005) Biodegradable polymers and their layered silicate nanocomposites: In greening the 21st century materials world. Progress in Materials Science, 50, 962-1079.

Salamone, J.C. (1996) Polymeric Materials Encyclopedia. USA: CRC Press, Inc.

Sasic, S., Kita, Y., Furukawa, T., Watari, M., Sieslere, H. W., and Ozaki, Y. (2000) Analyst, 125, 2315-2321.

Sudesh, K., Abe, H., and Doi, Y. (2000) Synthesis, structure and properties of polyhydroxyalkanoates: biological polyesters. Progress in Polymer Science, 25, 1503-1555.

Suzuki, S., Ohaki, M., Ichiyanagi, M., and Ozawa, M. (1998) Preparation of needle-like hydroxyapatite. Journal of Material Science Letter, 17, 381-383.

Storey, R.F., and Sherman, J.W. (2002) Kinetics and mechanism of the stannous octoate-catalyzed bulk polymerization of ε-Caprolactone. Macromolecules, 35, 1504-1512.

Stridsberg, K.M., Ryner, M., Albertsson, A.-C. (2002) Controlled Ring- Opening Polymerization: Polymers with Designed Molecular Architecture. Advance in Polymer Science, 157, 41-65.

Vergnes, B., Berzin, F. (2006) Modeling of reactive systems in twin-screw extrusion: challenges and applications. Comptes Rendus Chimie, 9, 1409-1418.

Wang, Y., Li, Y., Luo, Y., Huang, M., and Liang, Z. (2009) Synthesis and characterization of a novel biodegradable thermoplastic shape memory polymer. Materials Letters, 63, 347-349.

Xiao, H., Lu, W., Yeh, J.T. (2009) Crystallization behavior of fully biodegradable poly(lactic acid)/poly(butylene adipate-co-terephthalate) blends. Journal of Applied Polymer Science. 112, 6, 3754-3763.

Young, F.K., Chang, N.C., Young, D.K., Ki, Y.L., and Moo, S.L. (2004) Compatibilization of Immiscible Poly(*l*-lactide) and Low Density Polyethylene Blends. Fibers and Polymers, 5, 270-274.

Zang, X., Macdonald, D.A., Goosen M.F.A., and Mcauley, K.B. (1994) Mechanism of lactide polymerization in the present of stannous octoate: The effect of hydroxyl and carboxylic acid substances. Journal of Polymer Science, 32, 2965-2970.

Zhu, W., Jaluria, Yo. (2004) Residence time and conversion in the extrusion of chemically reactive materials. Polymer Engineering and Science, 41, 1280-1291.

Zhu, Y., Wang, B., Gong, W., Kong, L., and Jia, Q. (2006) Investigation of the Hydrogen-Bonding Structure and Miscibility for PU/EP IPN Nanocomposites by PALS. Macromolecules, 39, 9441-9445.

APPENDICES

Appendix A Raw materials

Table A1 Melt Flow Rate (MFR) of raw materials (2.16 kg/230°C)

Materials	MFR (g/10 min)
Ethylene (vinyl acetate)	8
Polylactide	4

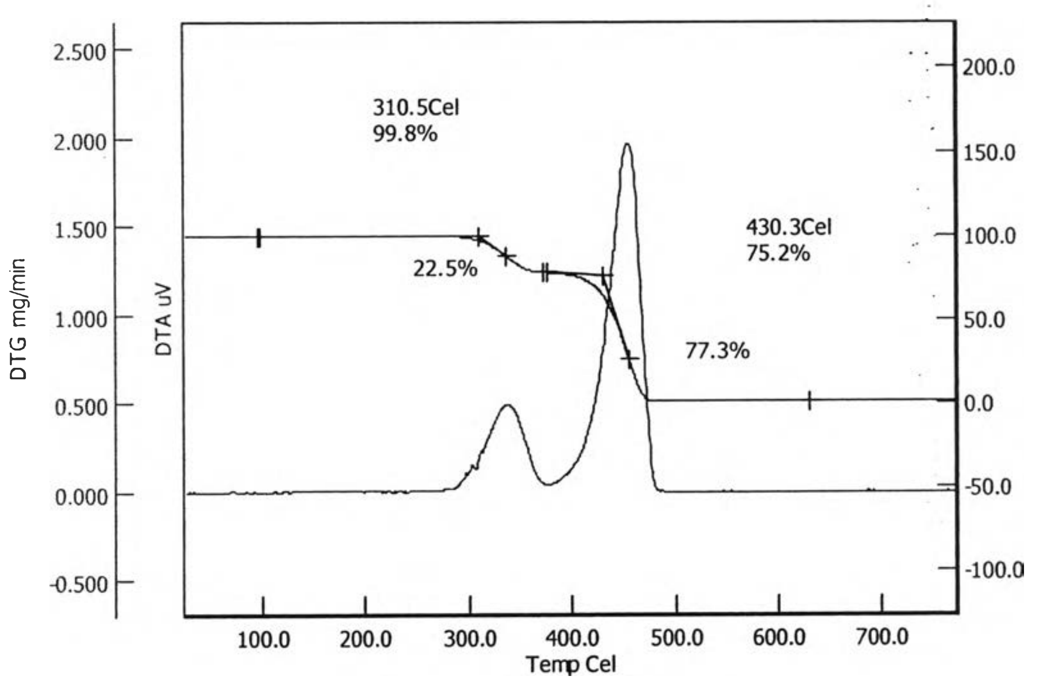

Figure A1 TGA thermogram of pure EVA.

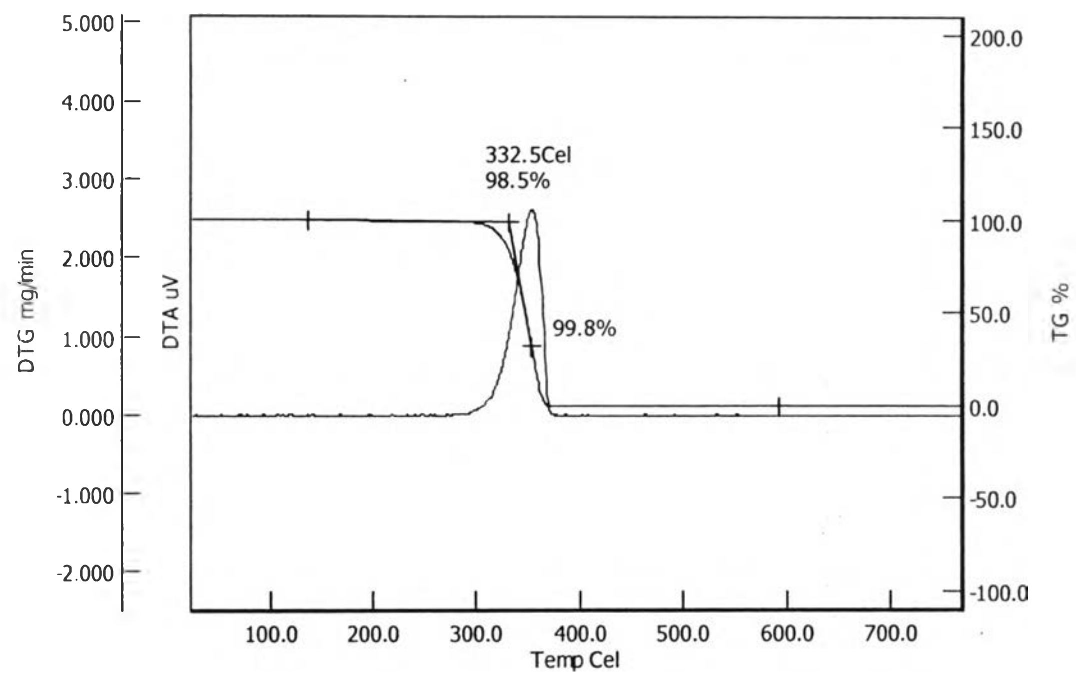

Figure A2 TGA thermogram of pure PLA.

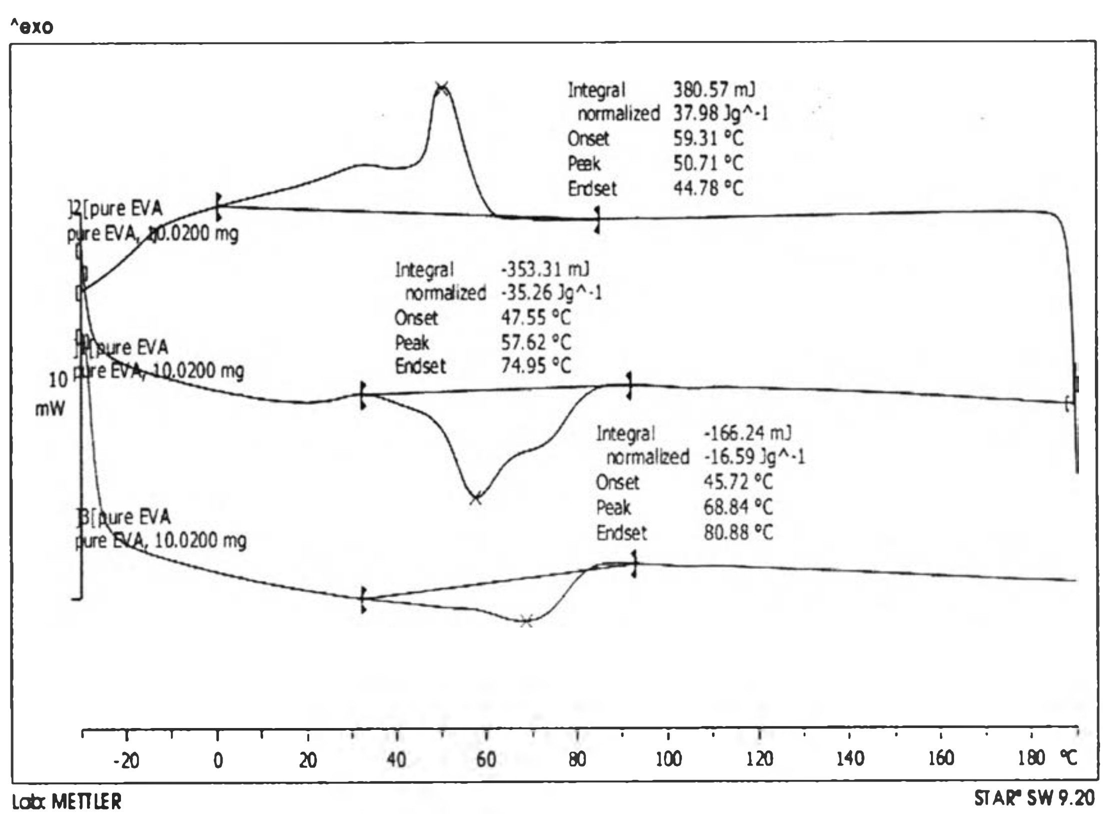

Figure A3 DSC thermogram of pure EVA.

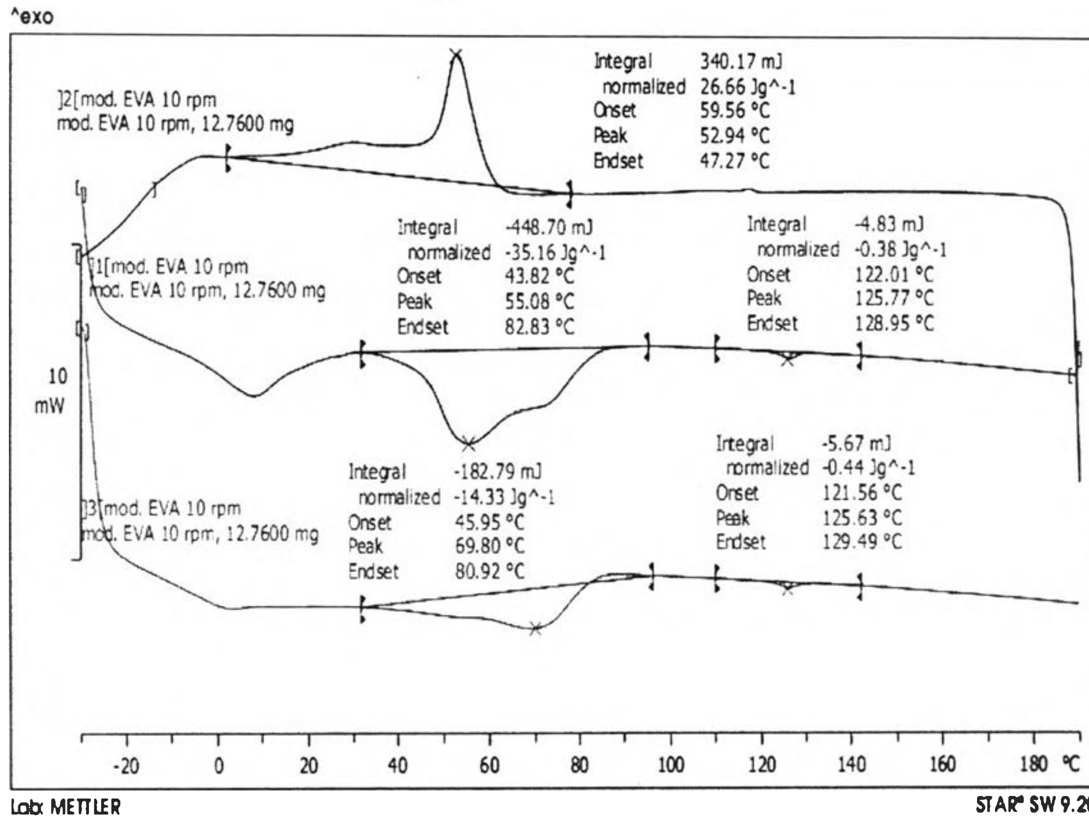

Figure A4 DSC thermogram of modified EVA (10 rpm).

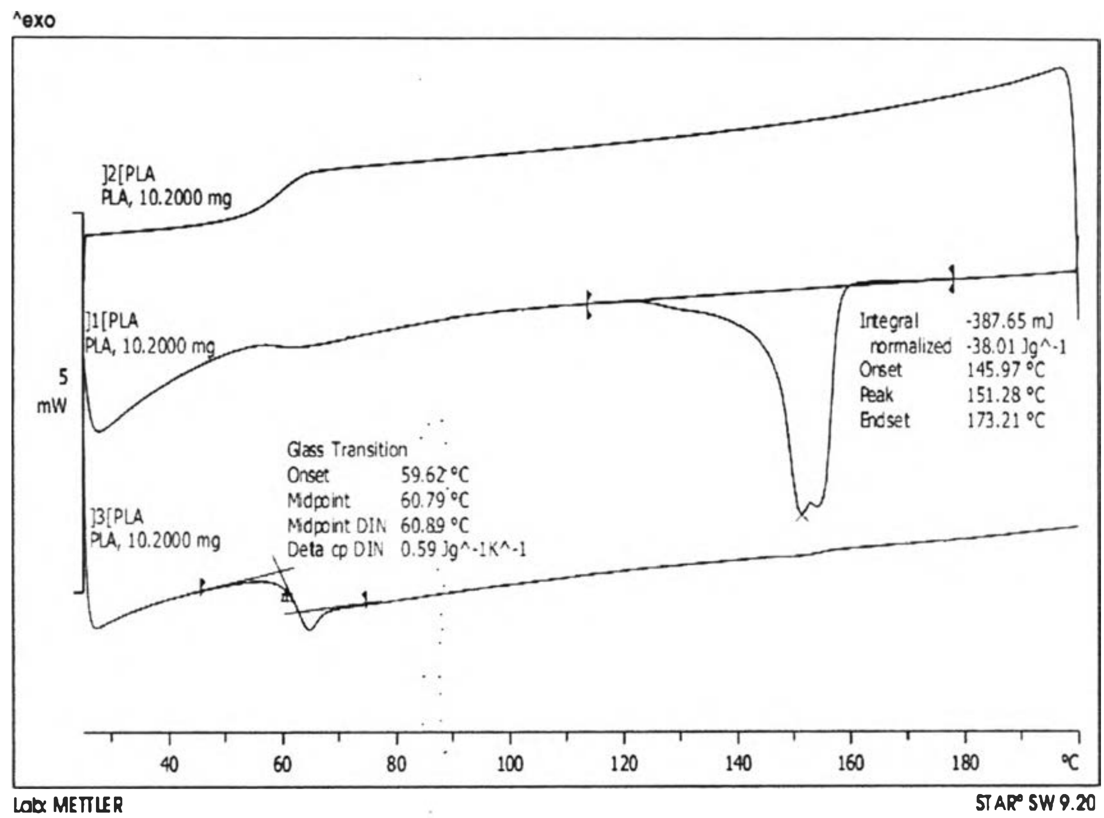

Figure A5 DSC thermogram of pure PLA.

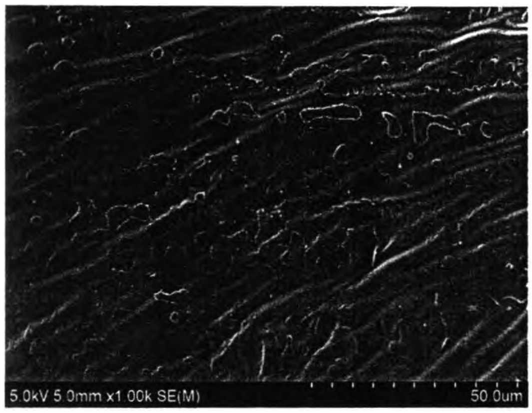

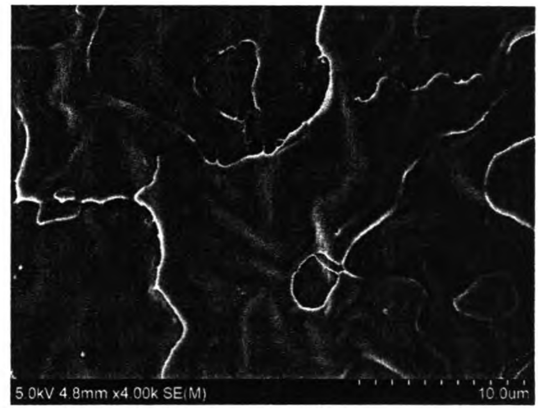

(a-1) 1000×   (a-2) 4000×

(a) Pure PLA

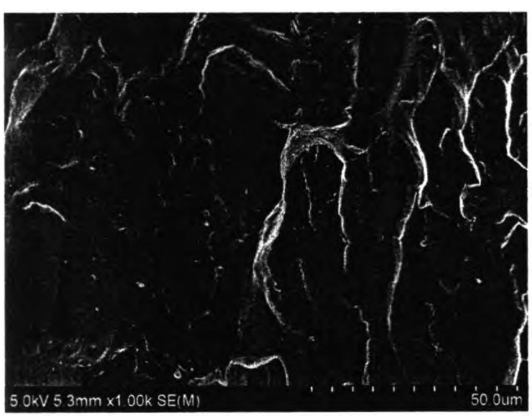

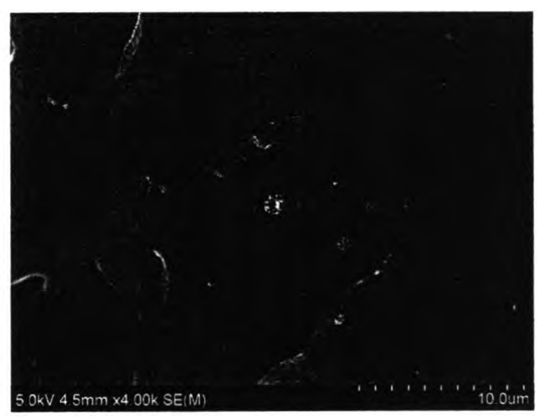

(b-1) 1000×   (b-2) 4000×

(b) Modified EVA

Figure A6 SEM images of (a) pure PLA and (b) modified EVA.

Appendix B EVA-g-PLA

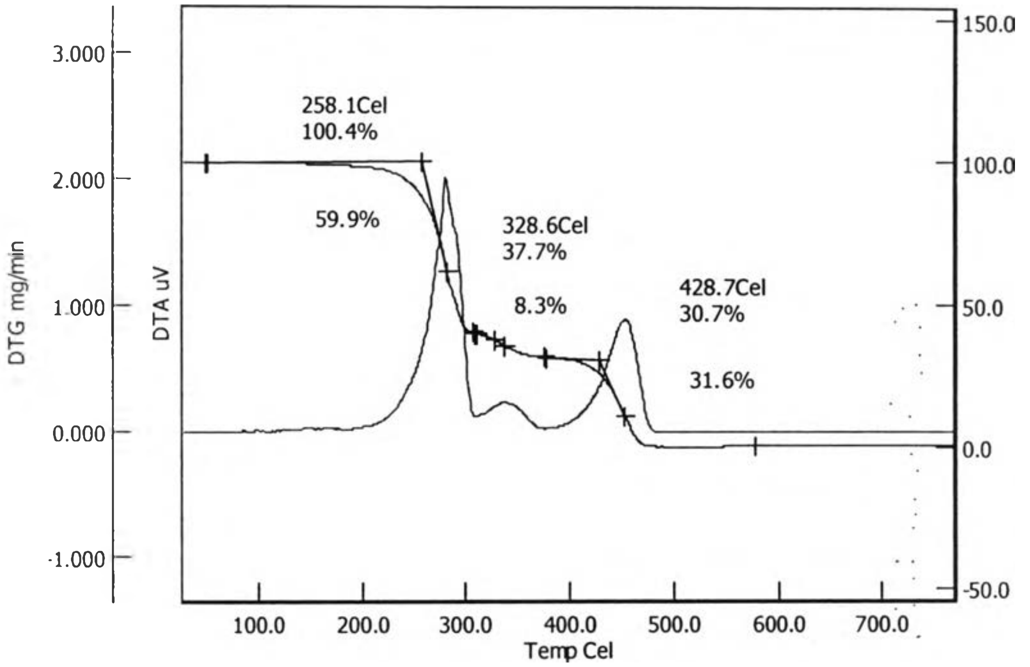

Figure B1 TGA thermogram of EVA-g-PLA (0.1%_30_2).

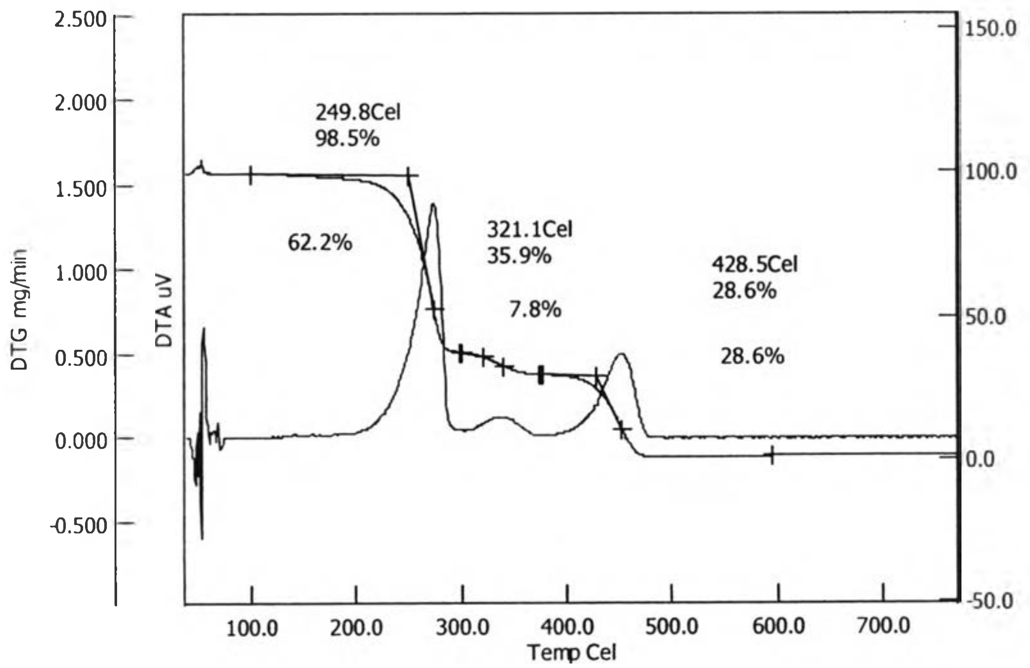

Figure B2 TGA thermogram of EVA-g-PLA (0.3%_30_2).

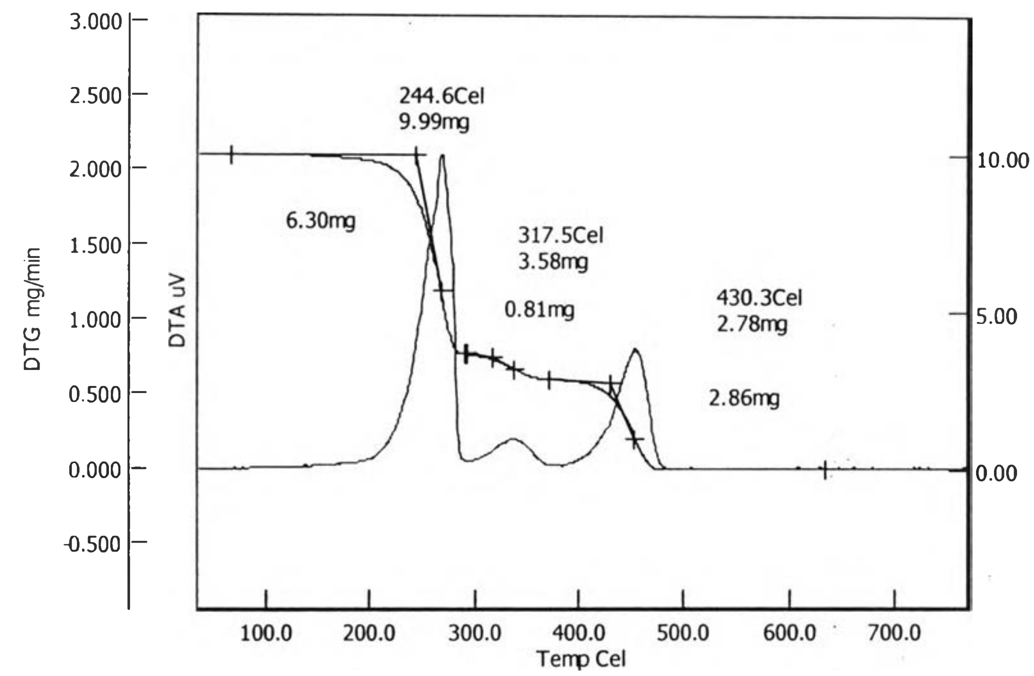

Figure B3 TGA thermogram of EVA-g-PLA (0.5%_30_2).

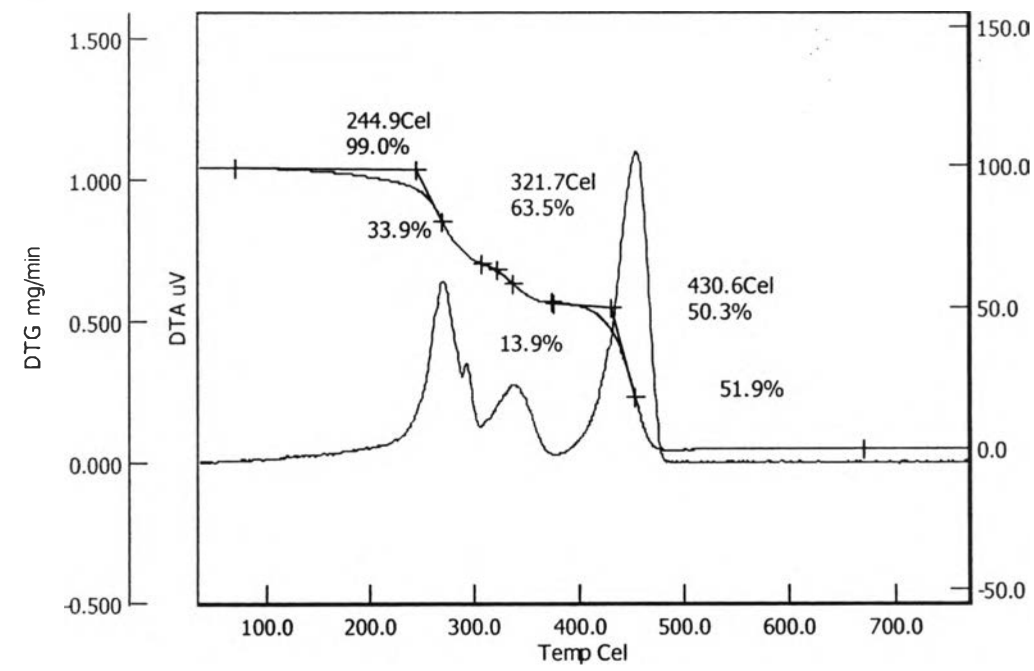

Figure B4 TGA thermogram of EVA-g-PLA (0.1%_30_3).

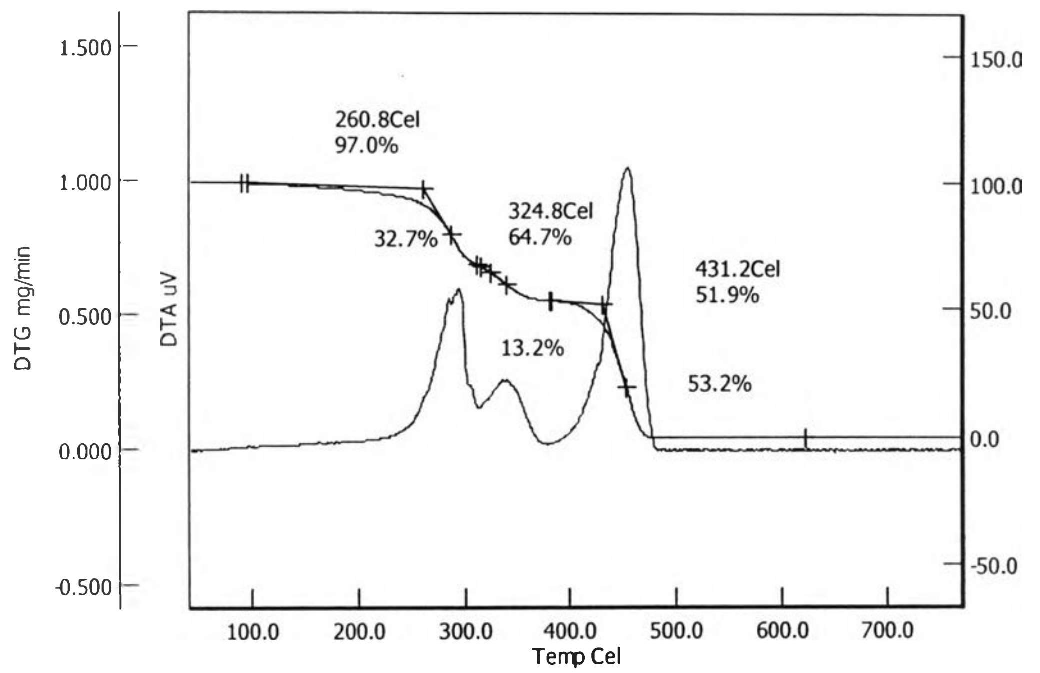

Figure B5 TGA thermogram of EVA-g-PLA (0.3%_30_3).

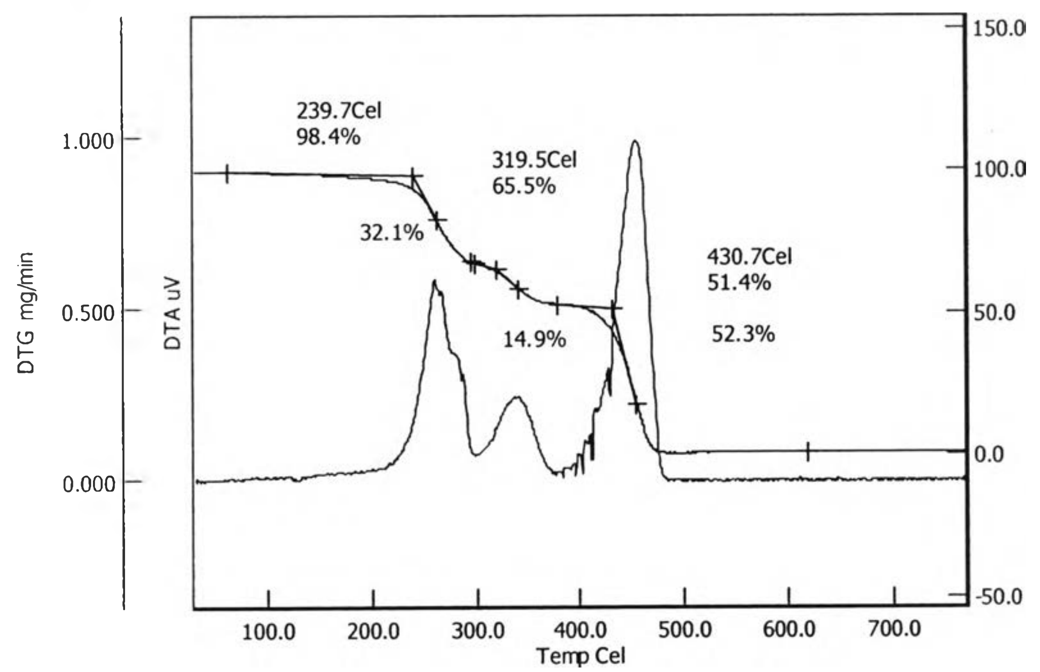

Figure B6 TGA thermogram of EVA-g-PLA (0.5%_30_3).

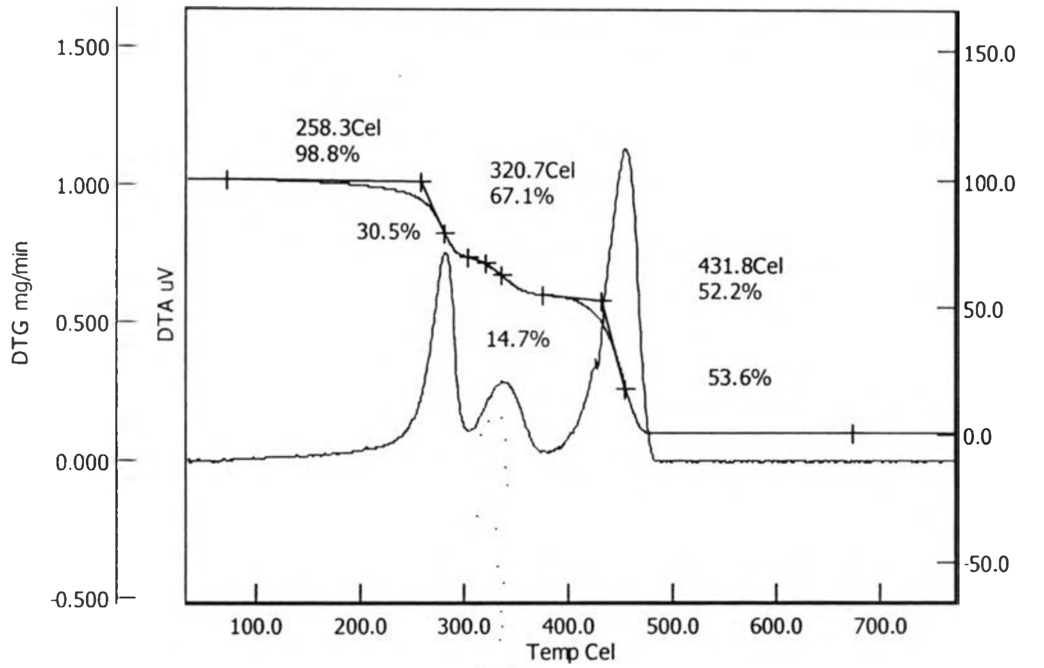

Figure B7 TGA thermogram of EVA-g-PLA (0.1%_40_2).

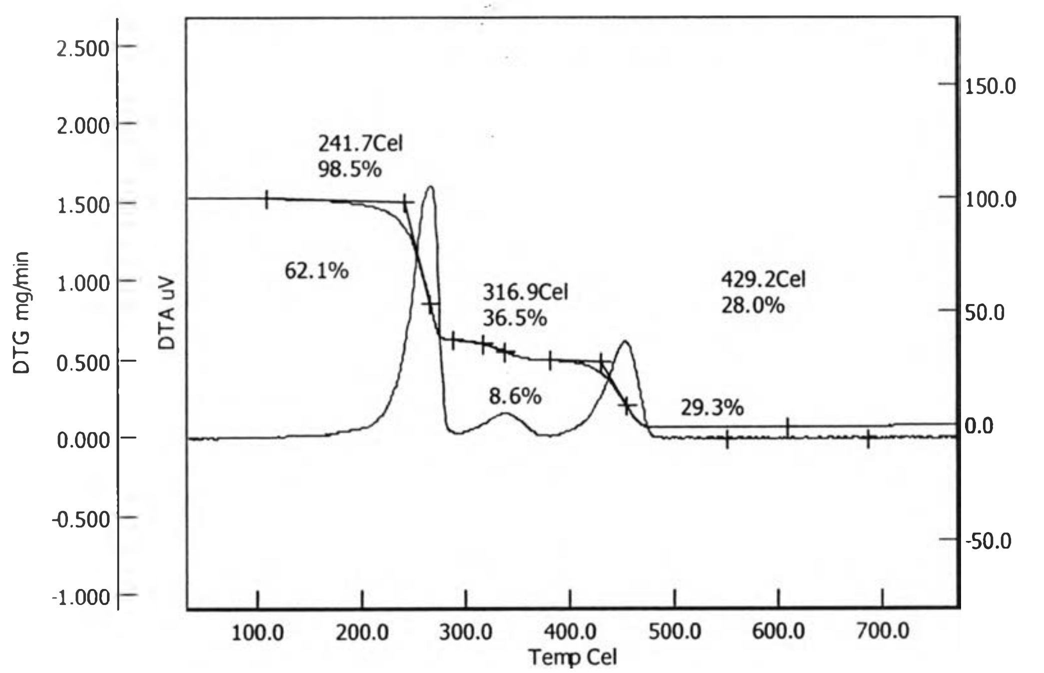

Figure B8 TGA thermogram of EVA-g-PLA (0.3%_40_2).

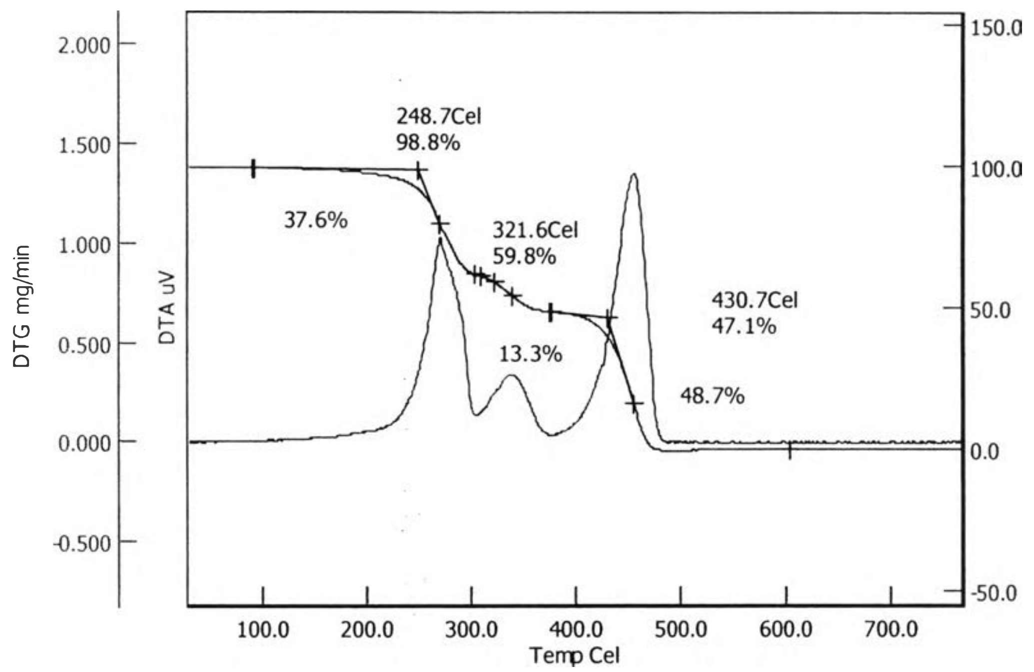

Figure B9 TGA thermogram of EVA-g-PLA (0.5%_40_2).

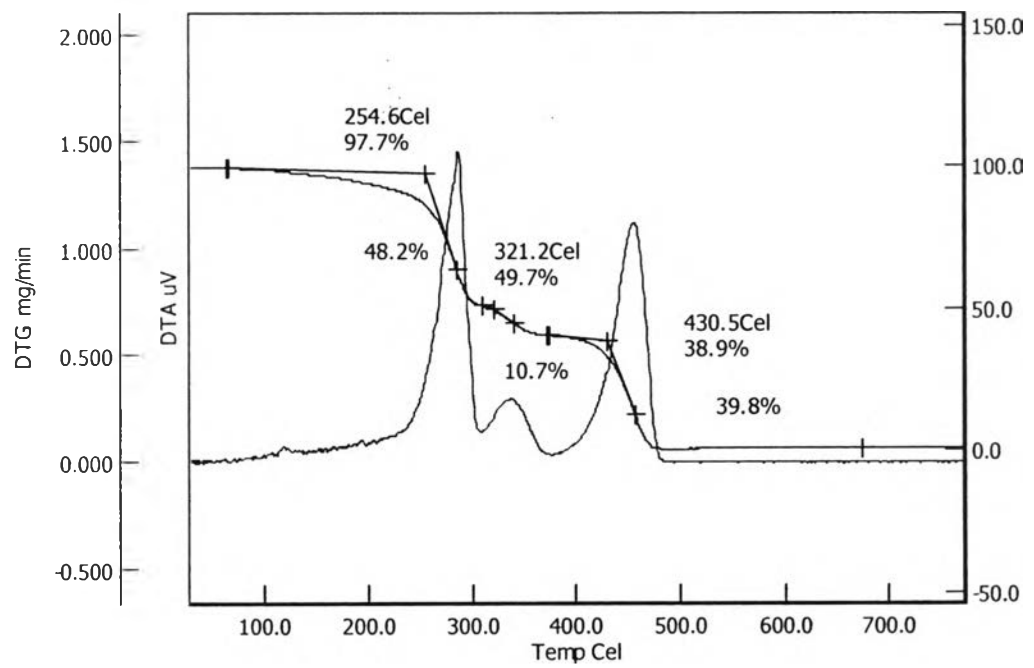

Figure B10 TGA thermogram of EVA-g-PLA (0.1%_40_3).

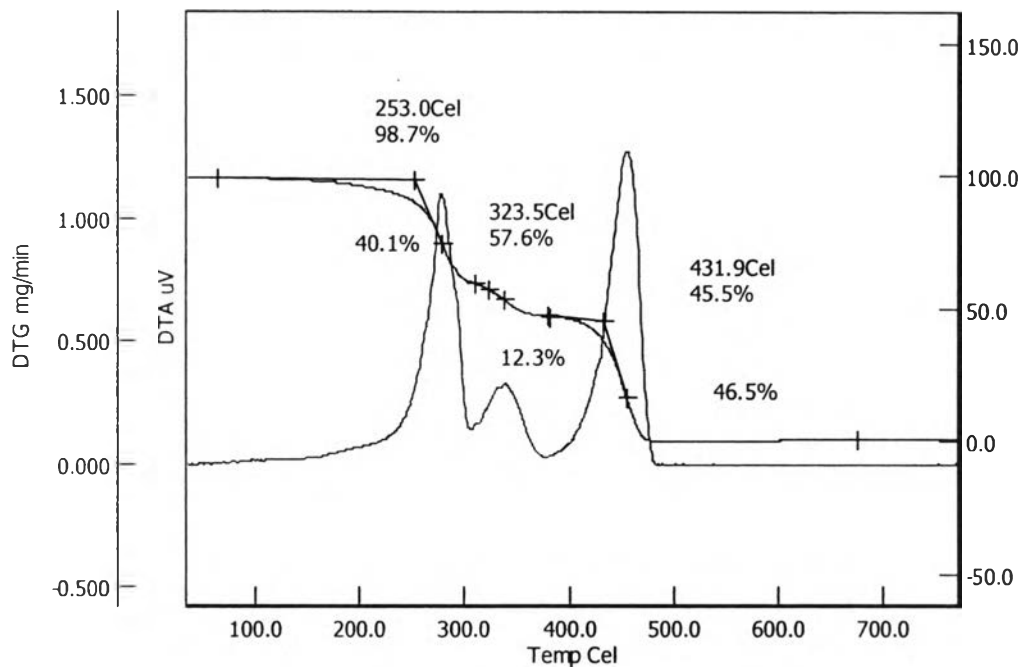

Figure B11 TGA thermogram of EVA-g-PLA (0.3%_40_3).

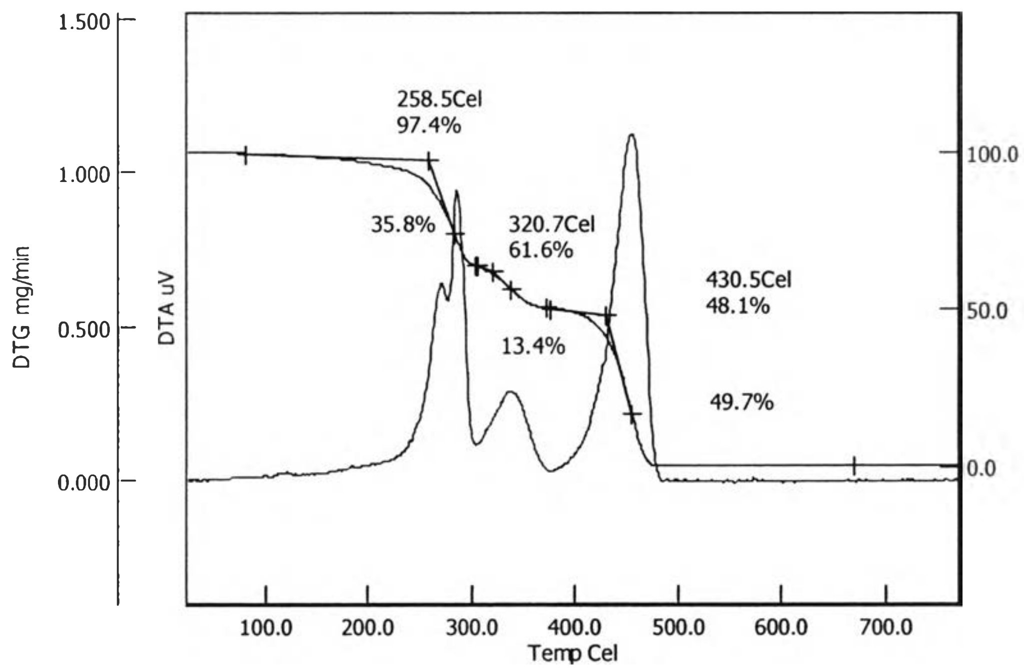

Figure B12 TGA thermogram of EVA-g-PLA (0.5%_40_3).

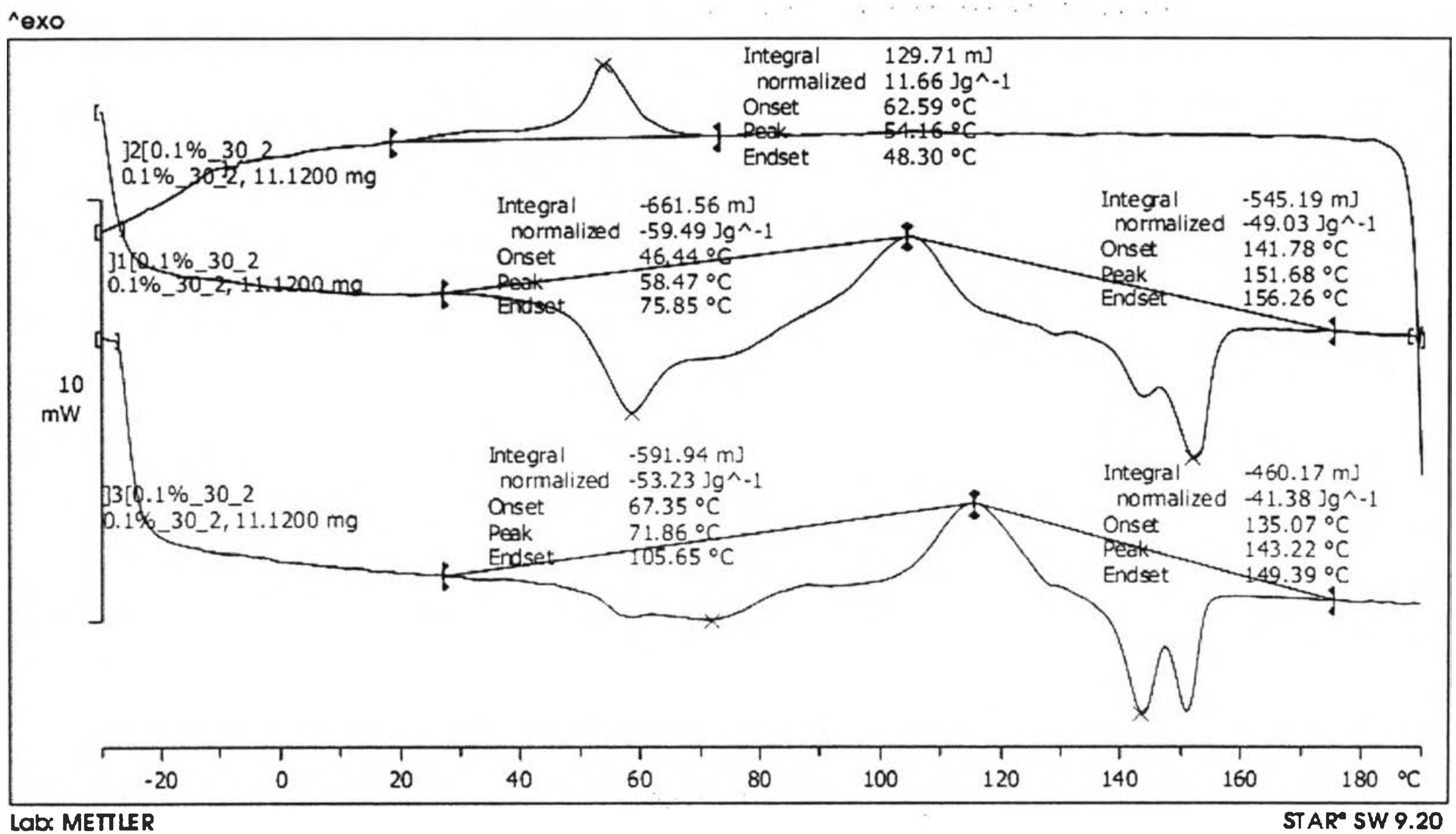

Figure B13 TGA thermogram of EVA-g-PLA (0.1%_30_2)

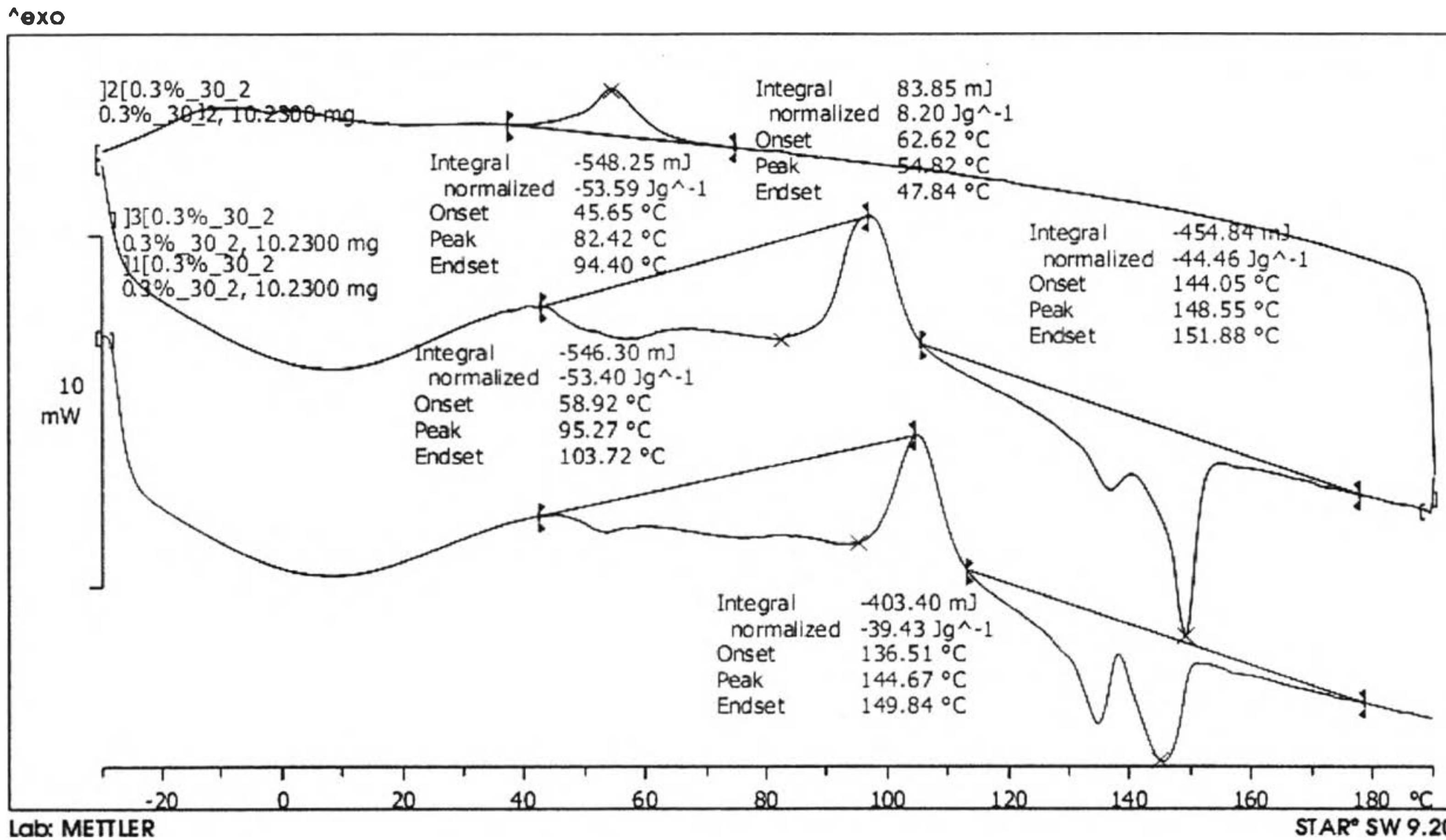

Figure B14 TGA thermogram of EVA-g-PLA (0.3%_30_2).

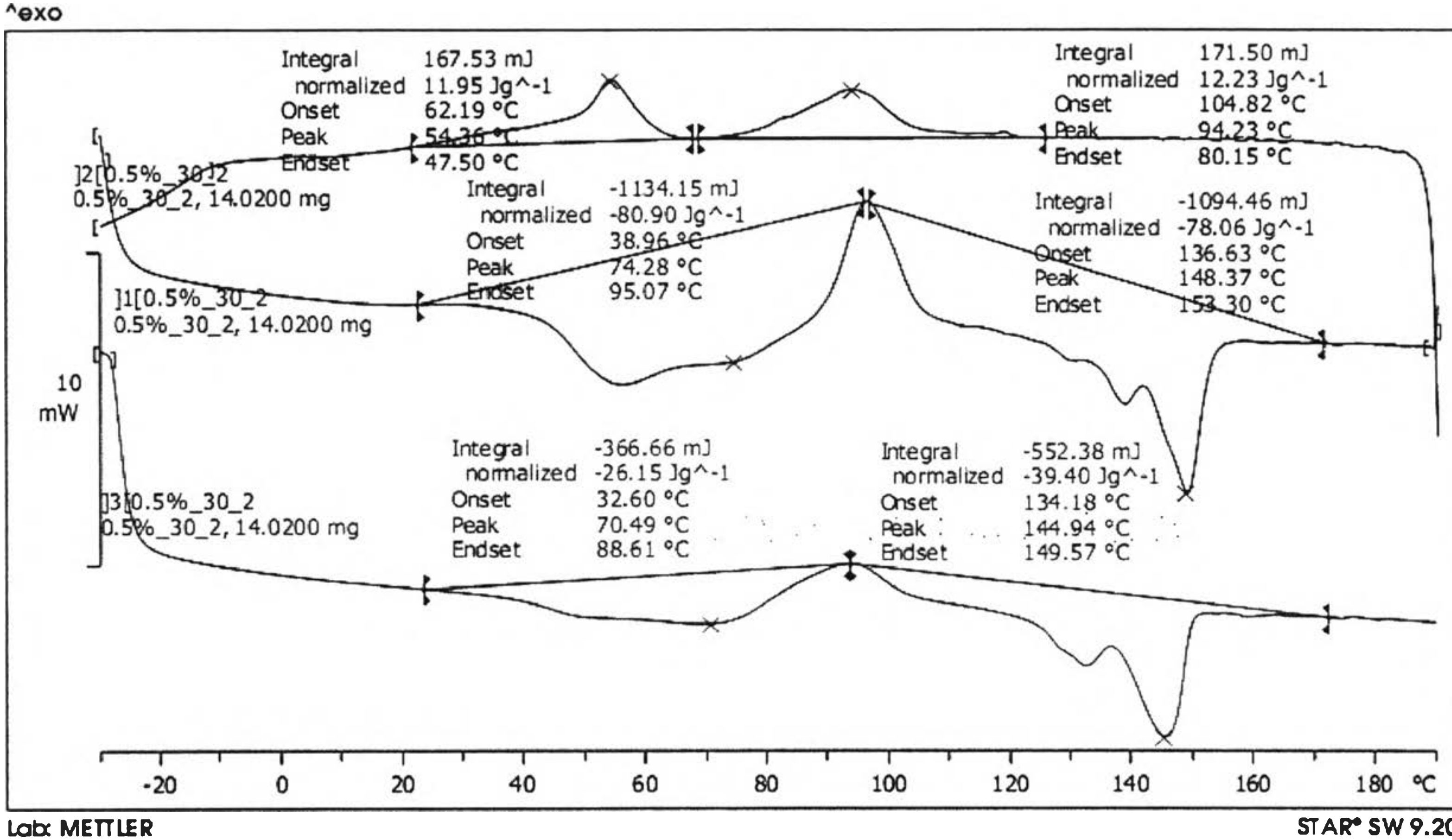

Figure B15 TGA thermogram of EVA-g-PLA (0.5%_30_2).

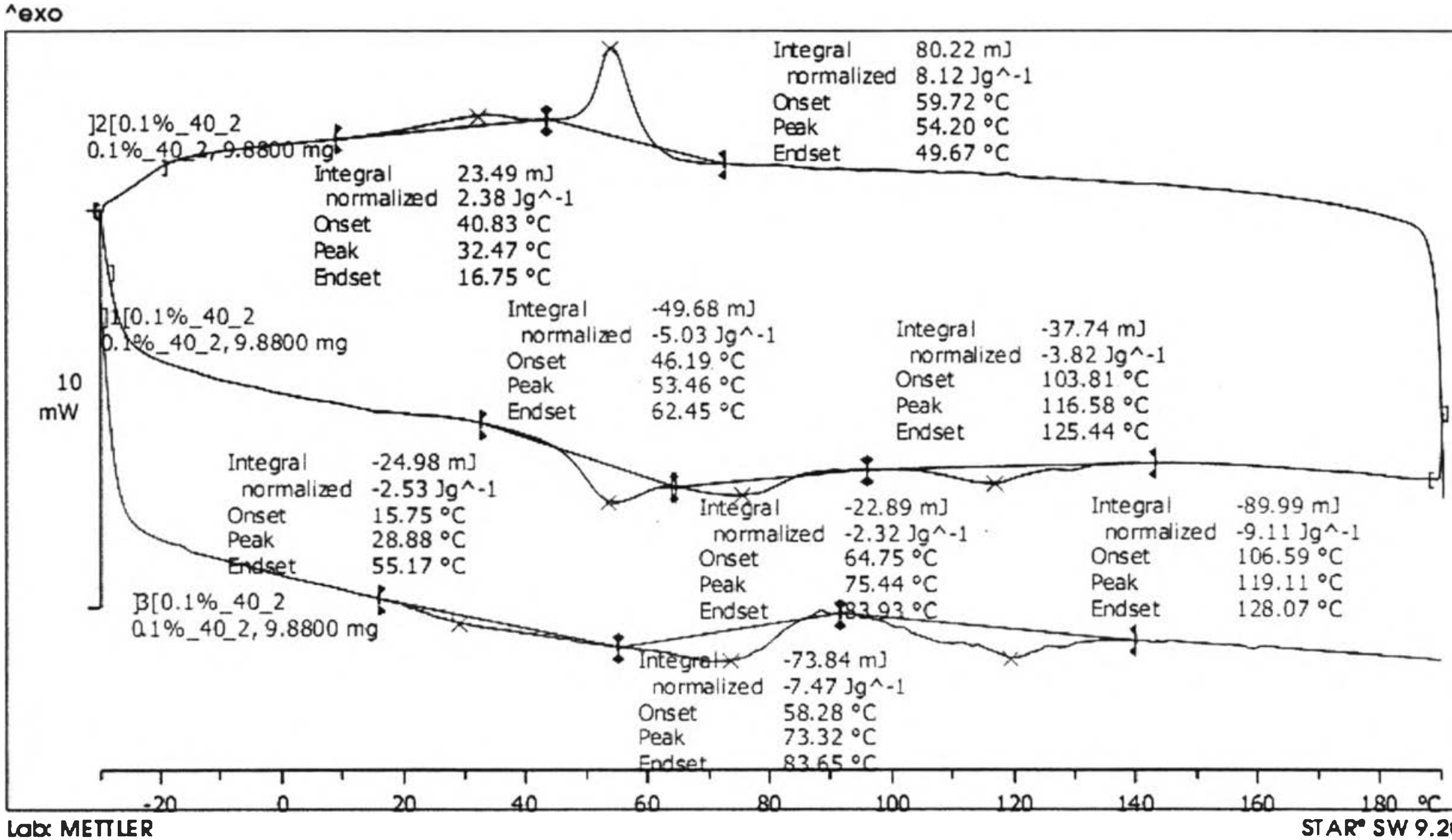

Figure B16 TGA thermogram of EVA-g-PLA (0.1%_40_2).

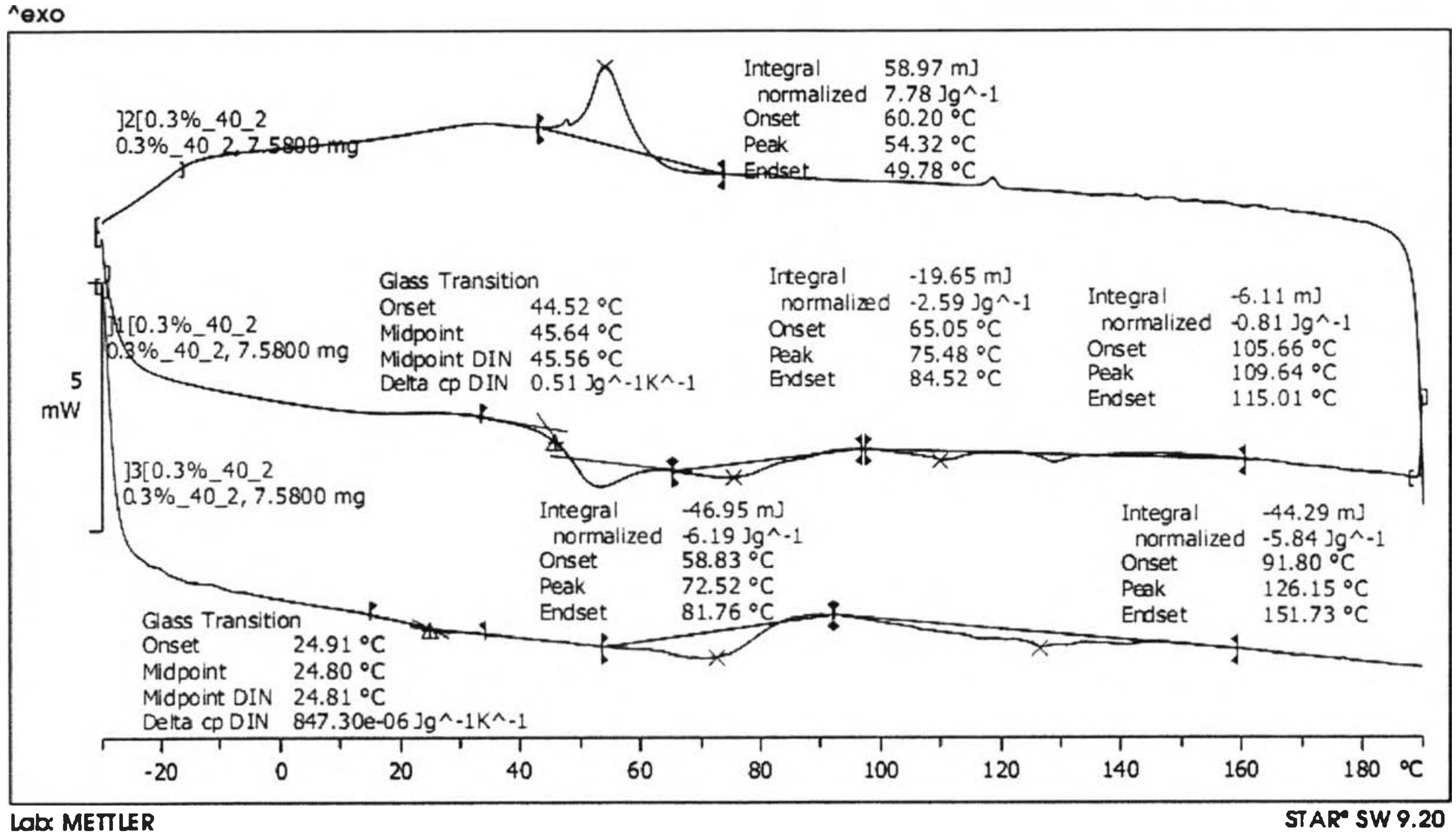

Figure B17 TGA thermogram of EVA-g-PLA (0.3%_40_2).

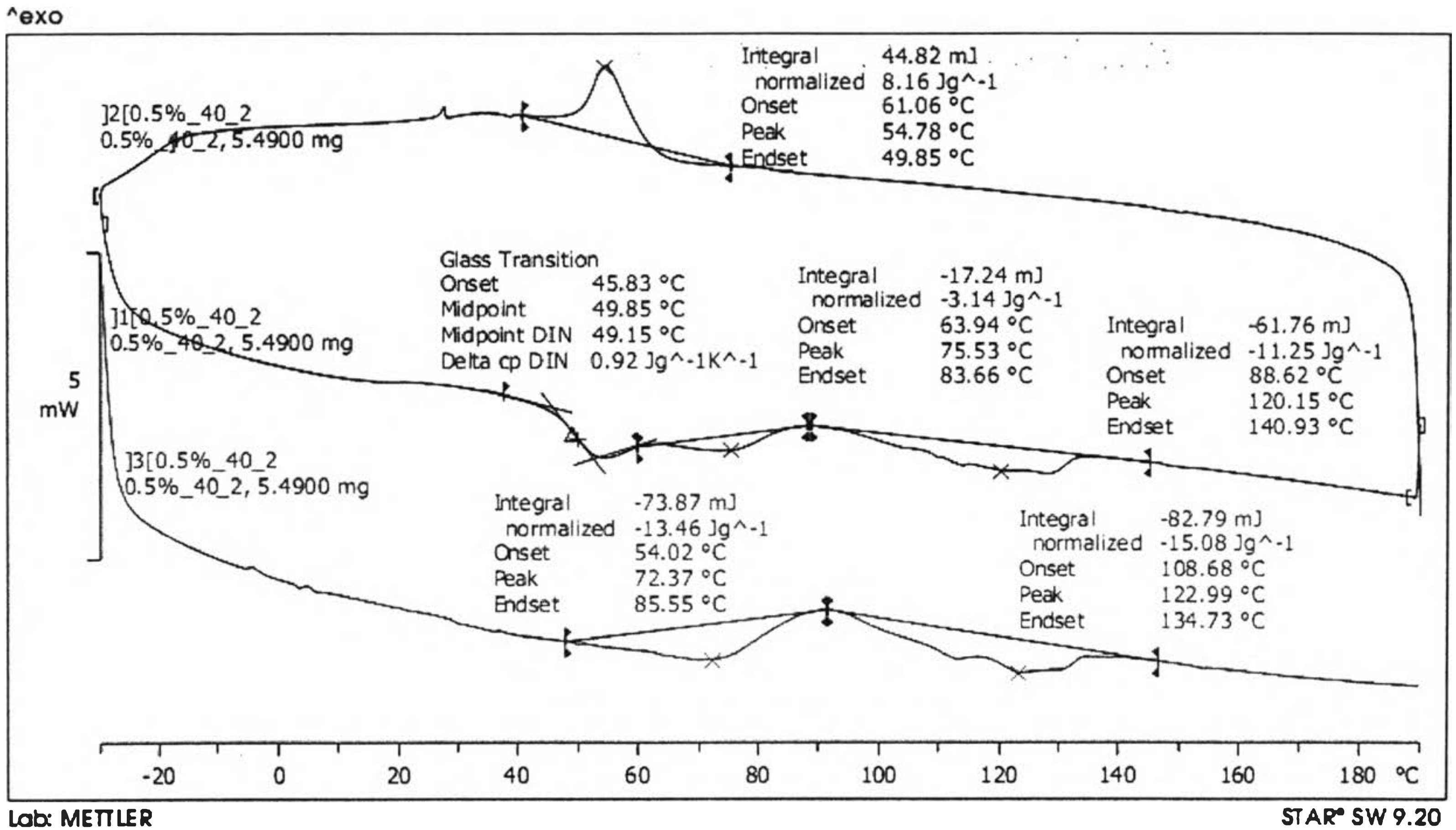

Figure B18 TGA thermogram of EVA-g-PLA (0.5%_40_2).

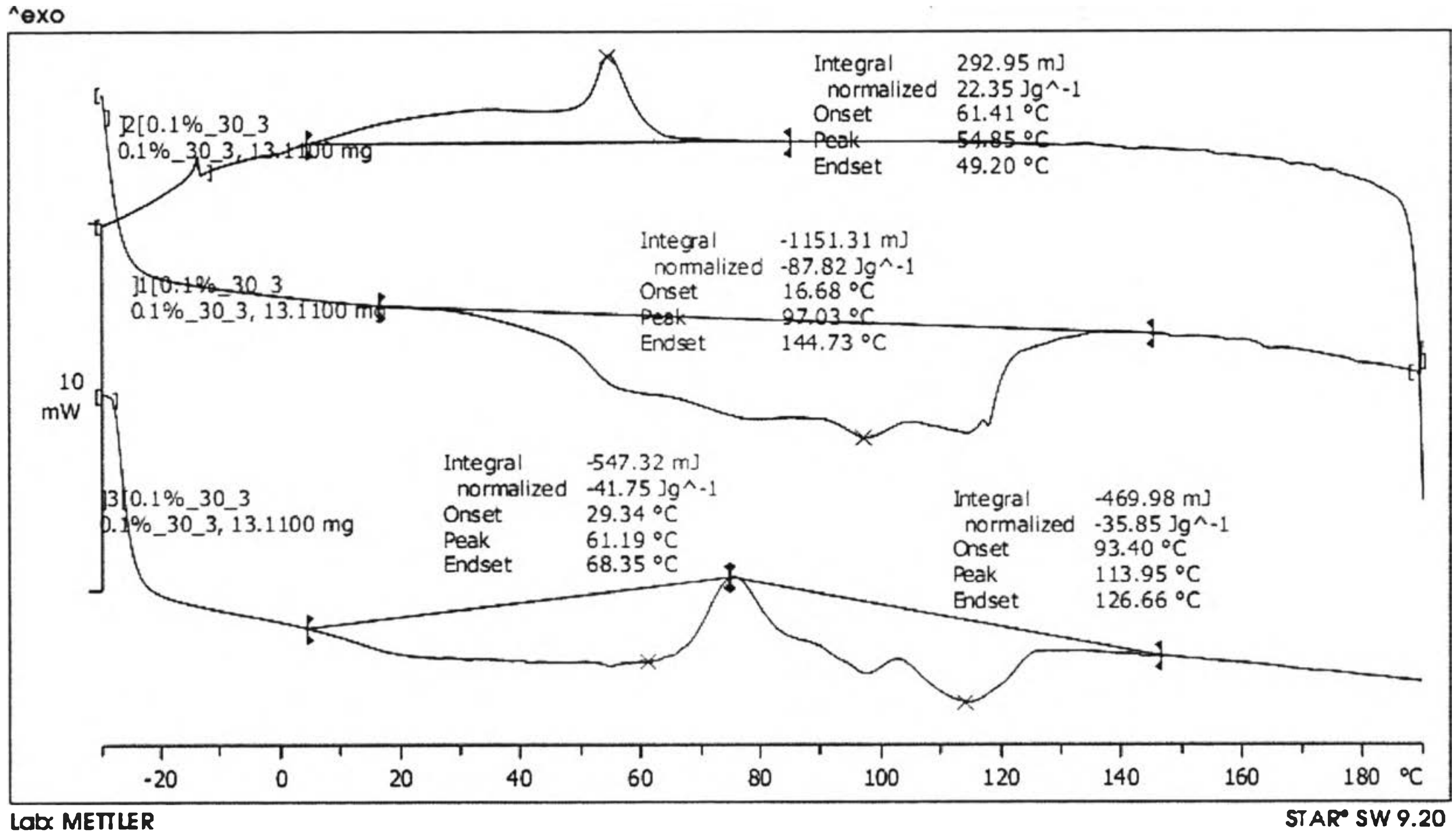

Figure B19 TGA thermogram of EVA-g-PLA (0.1%_30_3).

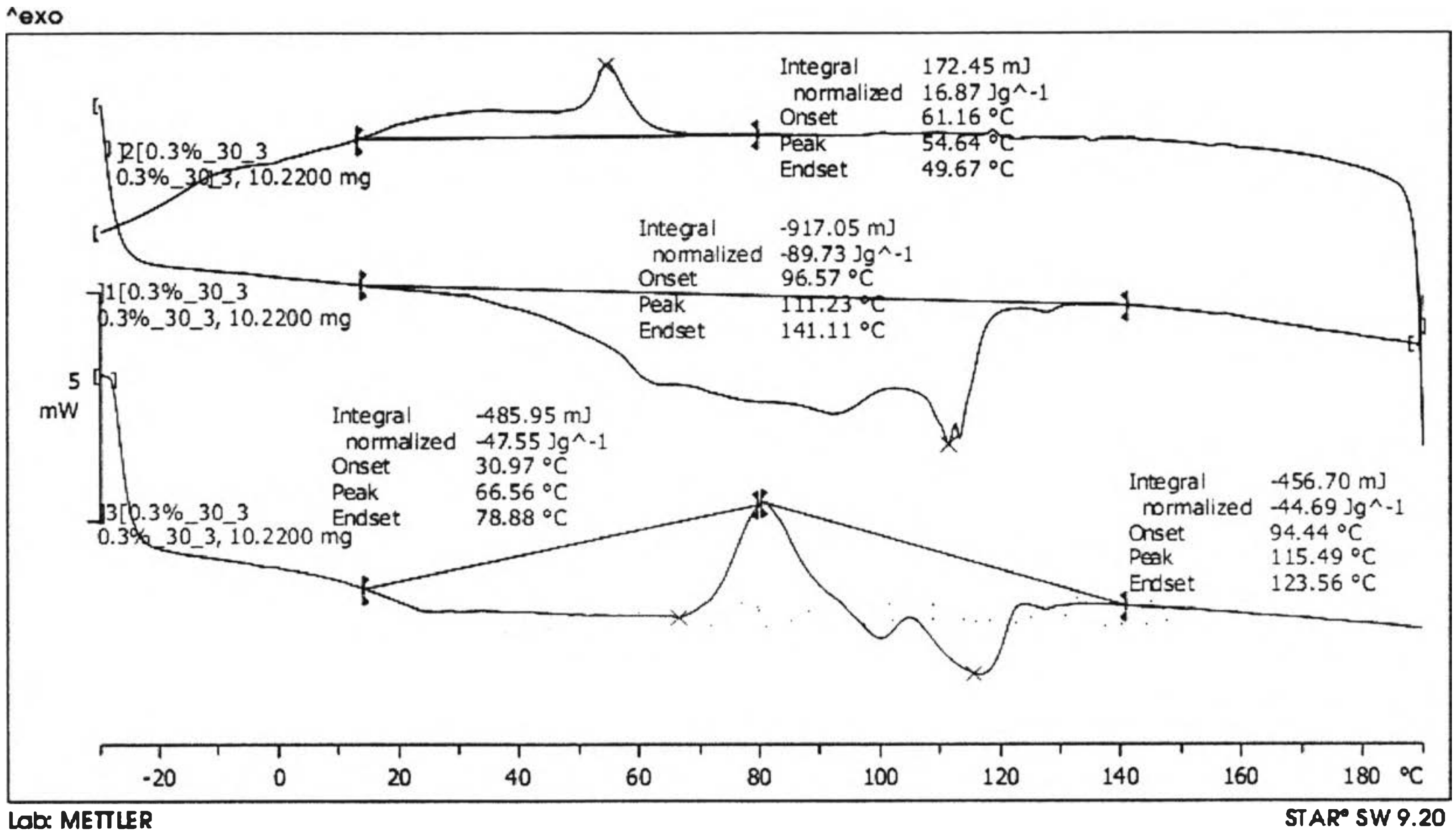

Figure B20 TGA thermogram of EVA-g-PLA (0.3%_30_3).

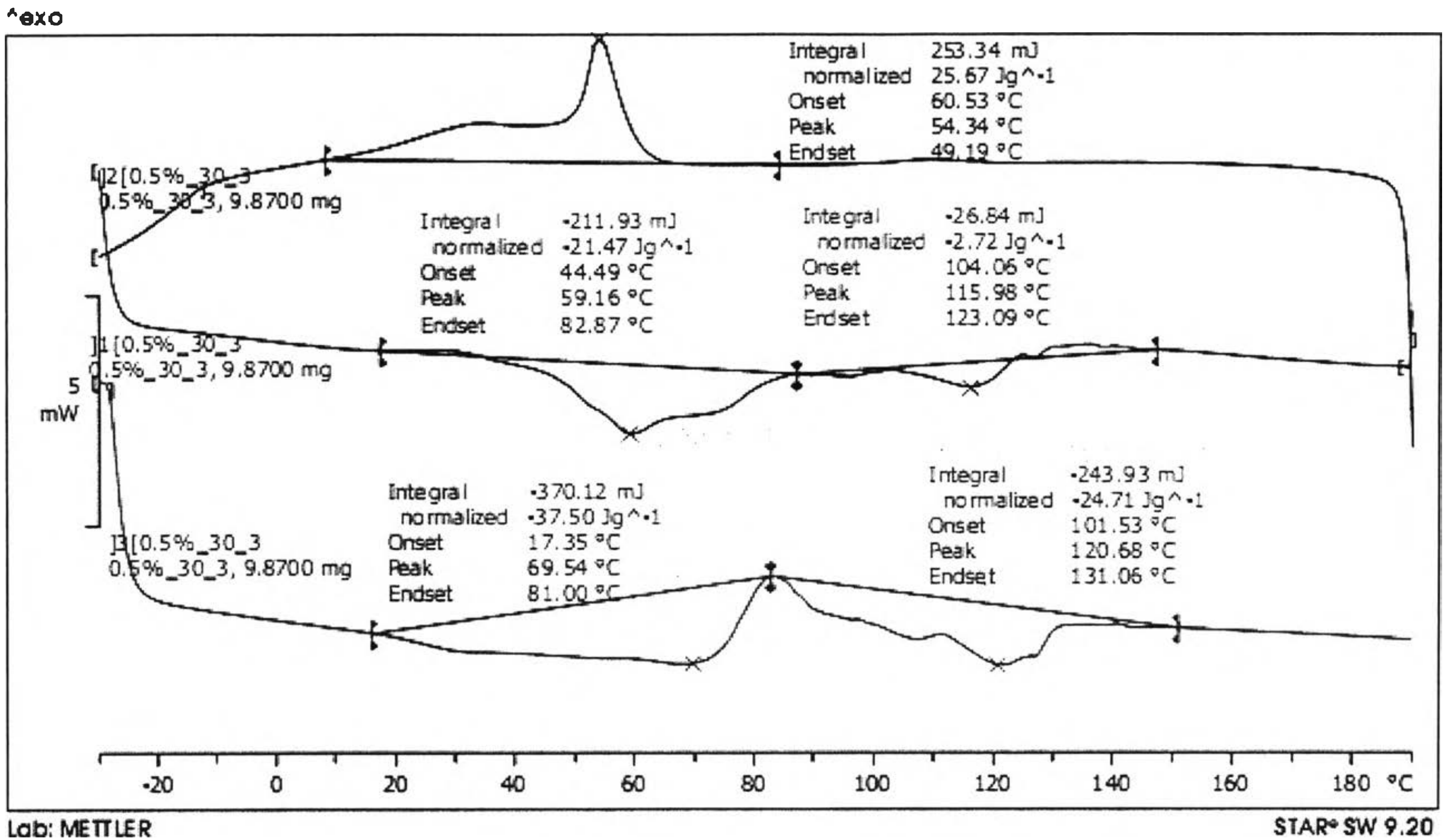

Figure B21 TGA thermogram of EVA-g-PLA (0.5%_30_3).

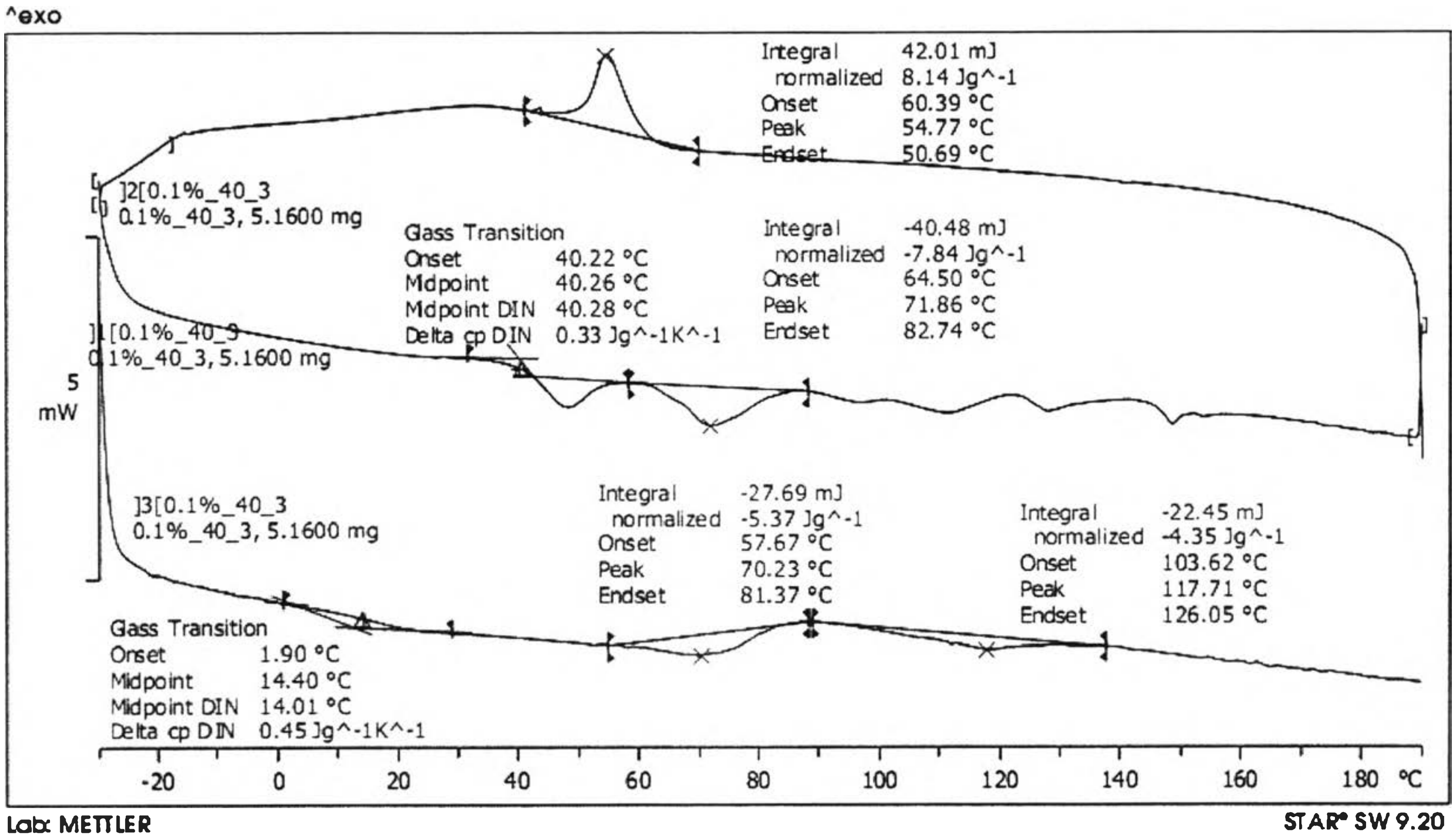

Figure B22 TGA thermogram of EVA-g-PLA (0.1%_40_3).

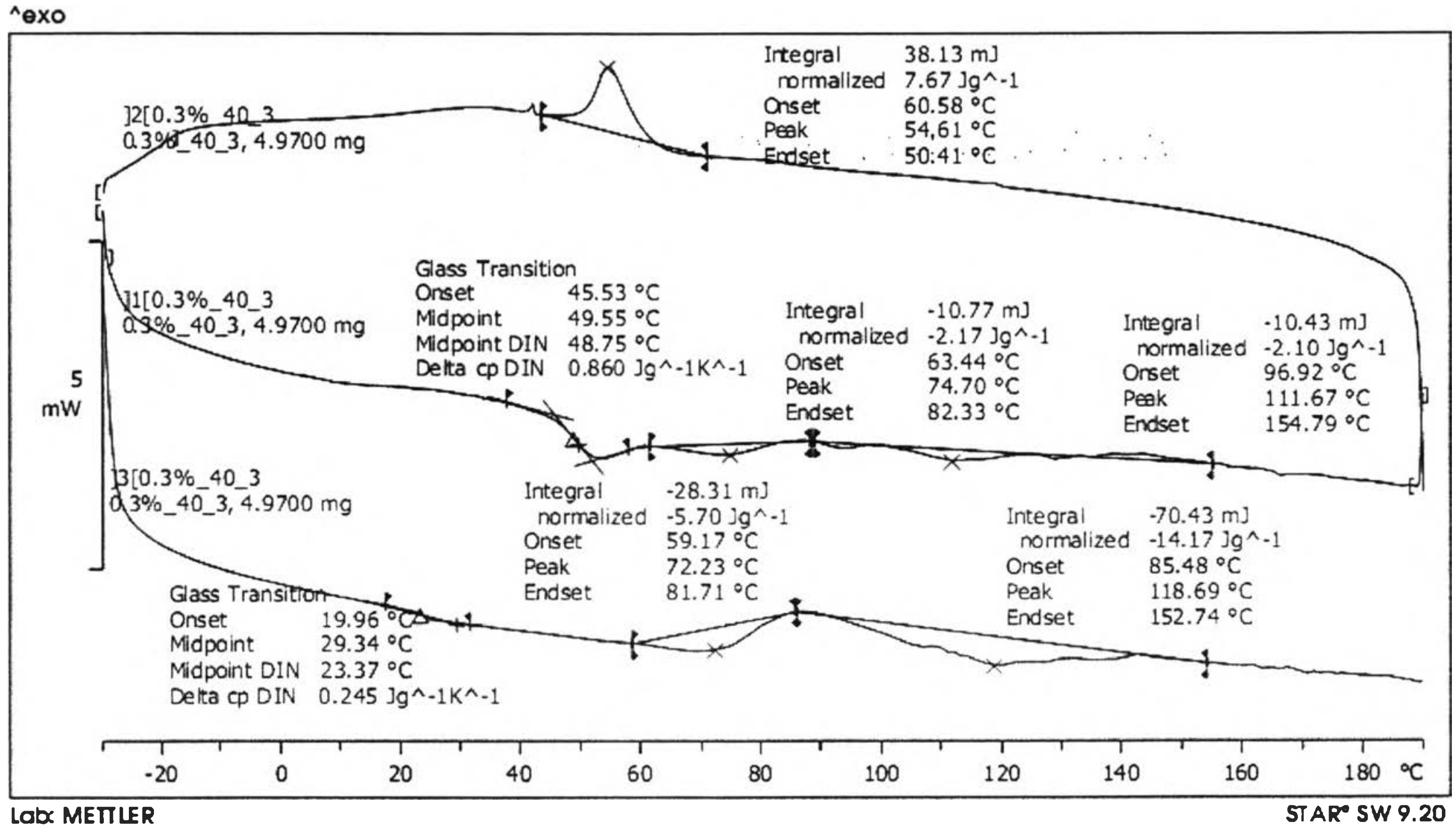

Figure B23 TGA thermogram of EVA-g-PLA (0.3%_40_3).

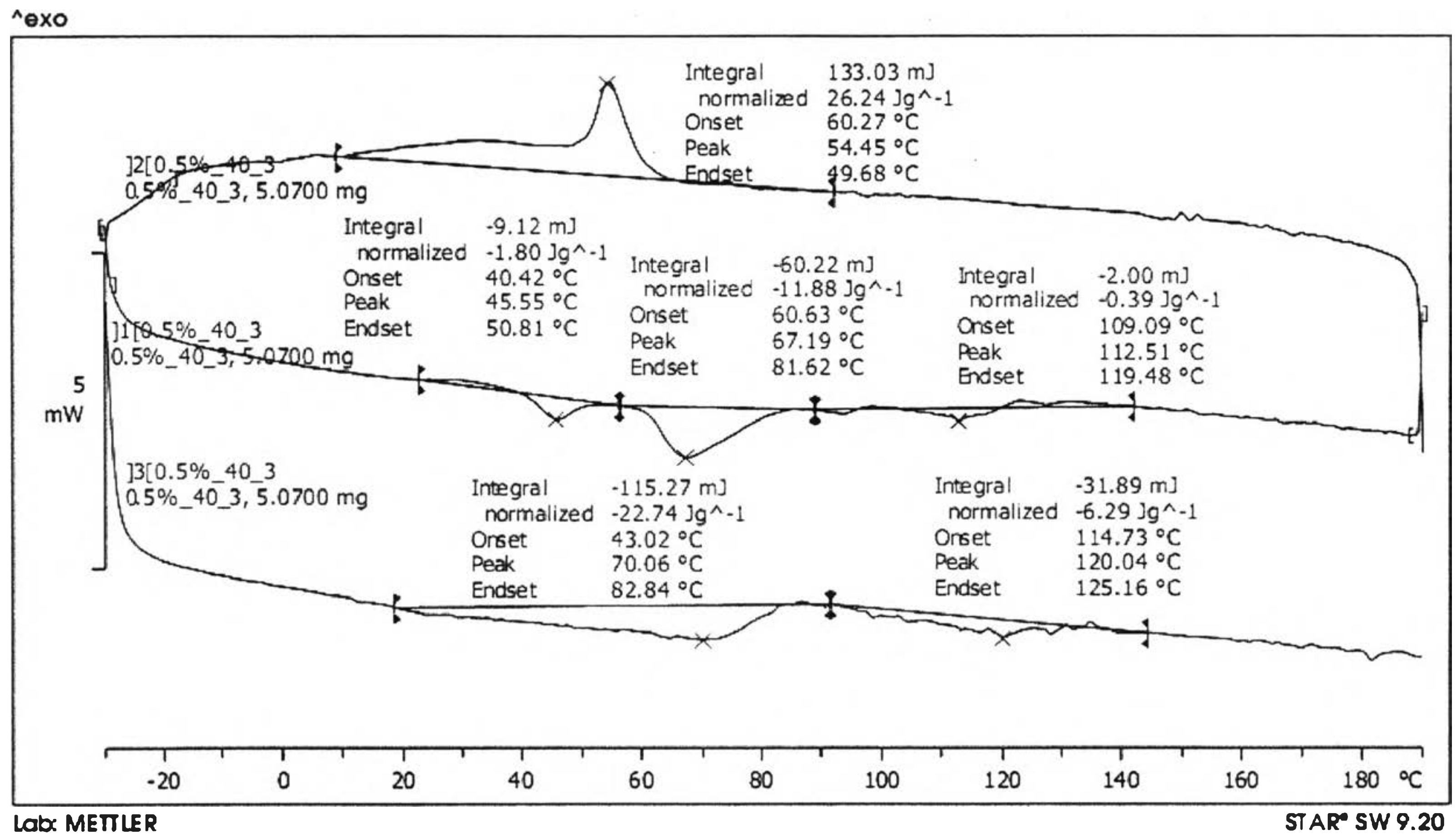

Figure B23 TGA thermogram of EVA-g-PLA (0.5%_40_3).

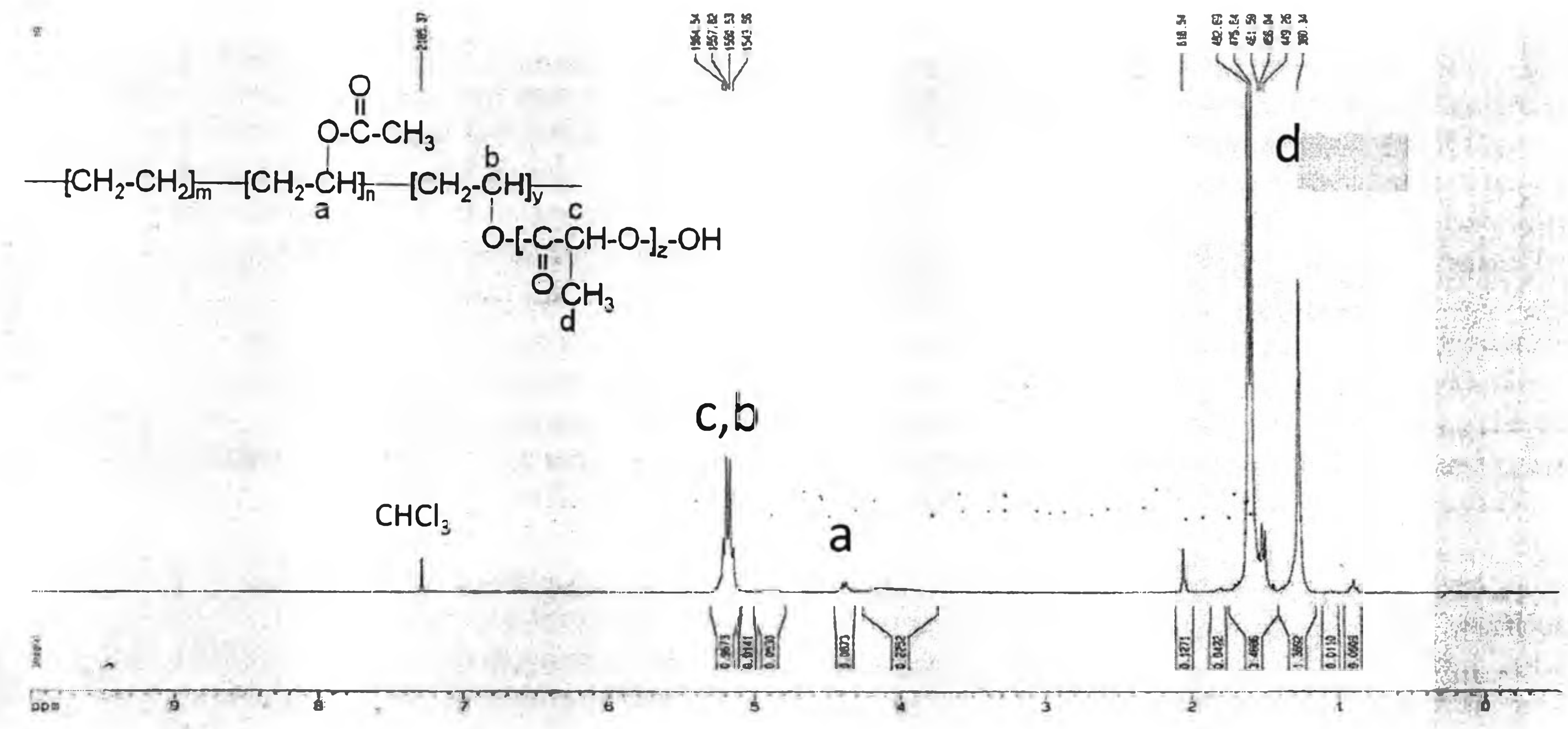

Figure B24 NMR spectrum of EVA-g-PLA.

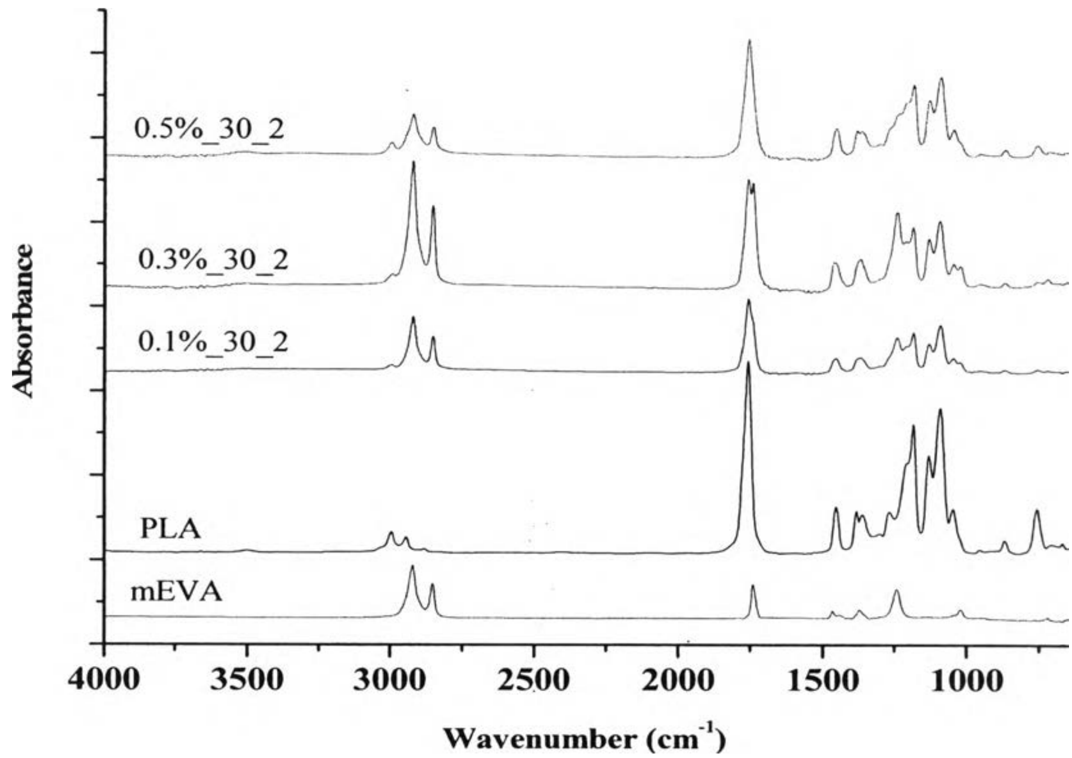

Figure B25 FTIR spectrum of EVA-g-PLA produced at 30 rpm (without LA).

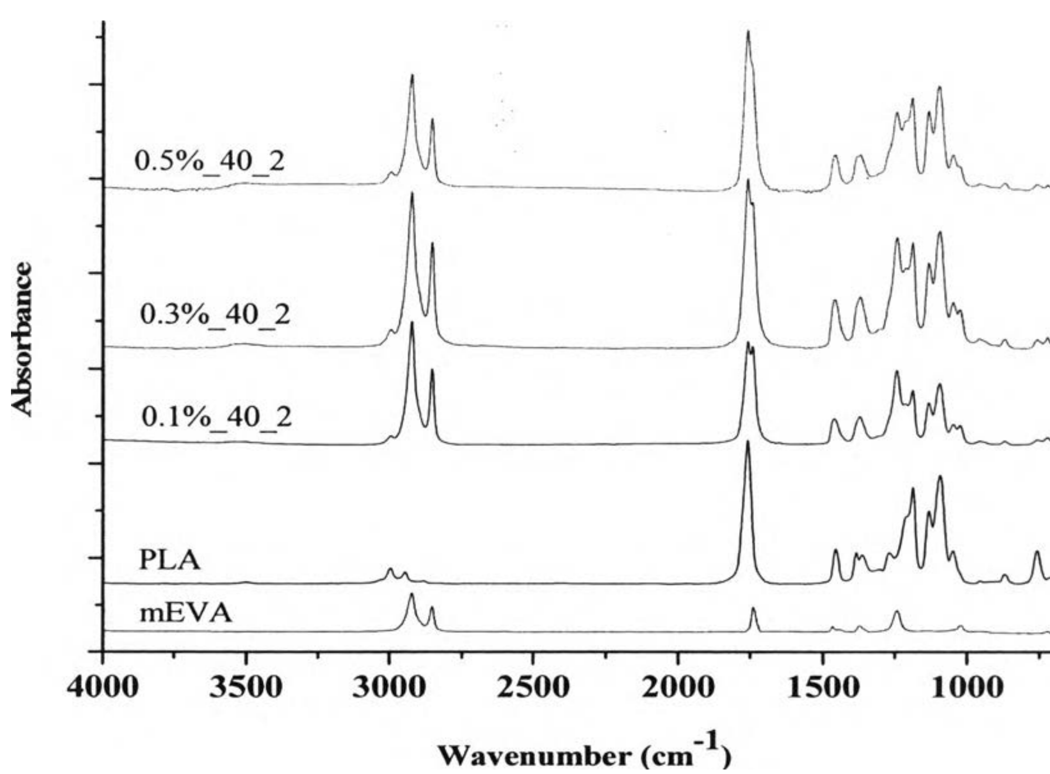

Figure B26 FTIR spectrum of EVA-g-PLA produced at 40 rpm (without LA).

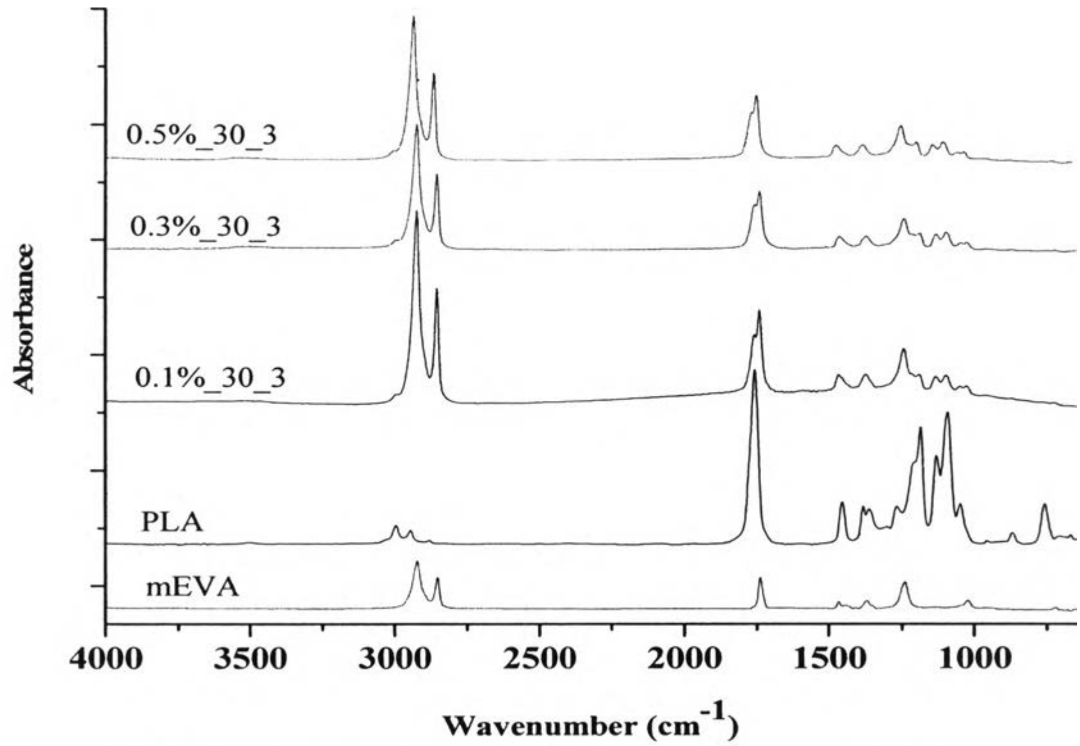

Figure B27 FTIR spectrum of EVA-g-PLA produced at 30 rpm (with LA).

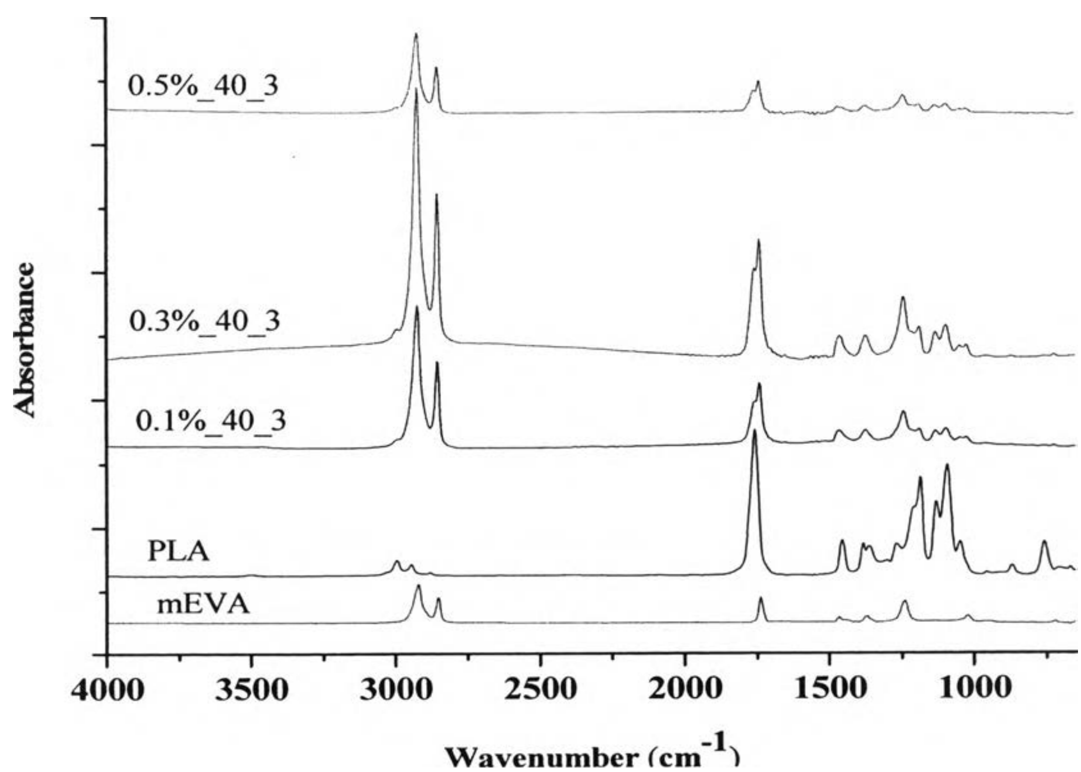

Figure B28 FTIR spectrum of EVA-g-PLA produced at 40 rpm (with LA).

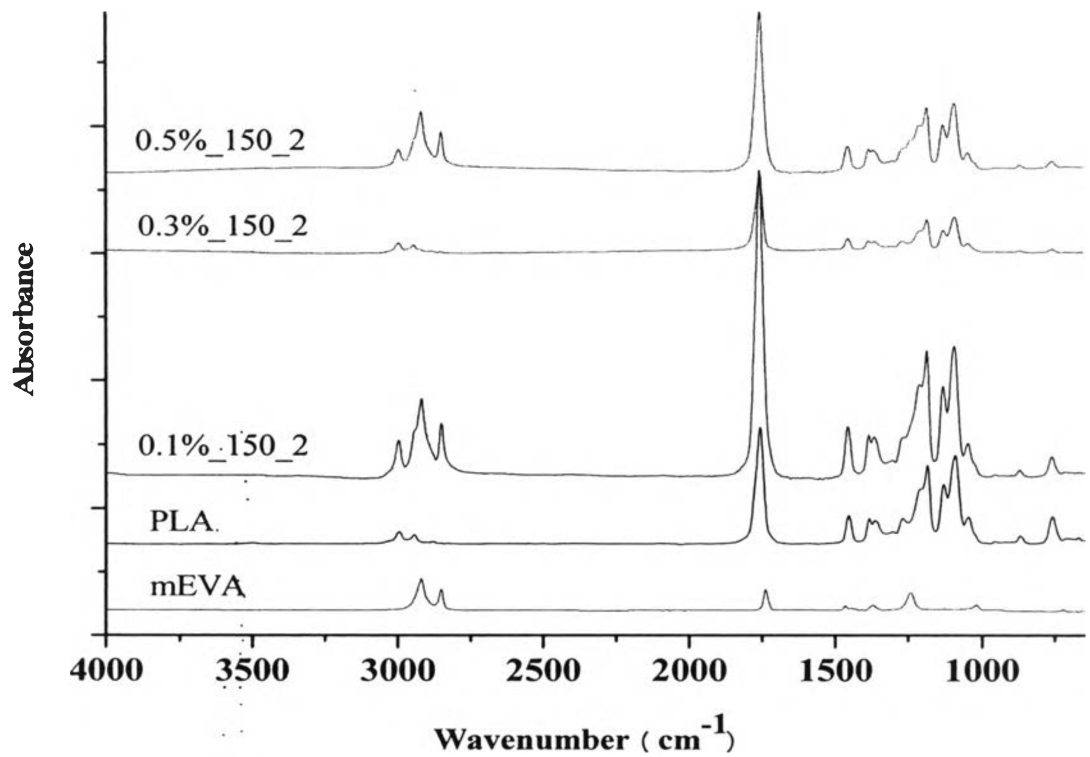

Figure B29 FTIR spectrum of EVA-g-PLA produced at 150 rpm (without LA).

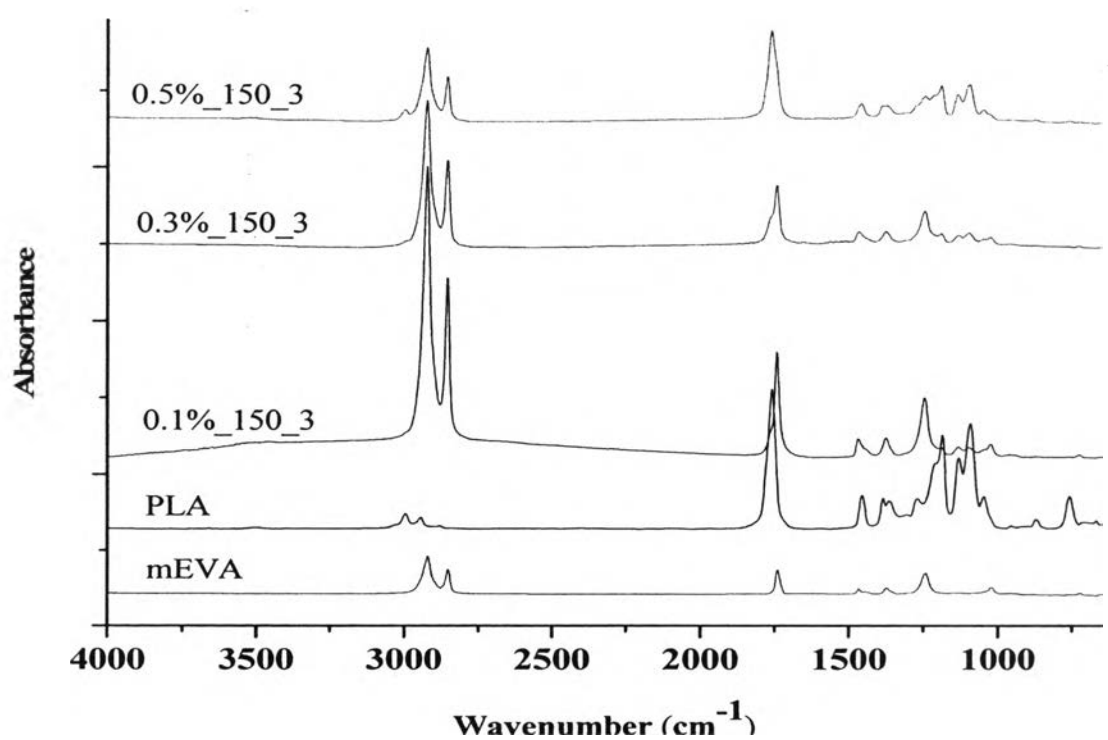

Figure B30 FTIR spectrum of EVA-g-PLA produced at 150 rpm (with LA).

Table B1 Viscosity ratio of EVA-g-PLA from Ubbelohde tube

Sample	time	viscosity ratio (t_1/t_0)
Chloroform	1.25	1
PLA	1.27	1.016
mod EVA	1.3	1.04
0.1%_30_2	1.31	1.048
0.3%_30_2	1.29	1.032
0.5%_30_2	1.29	1.032
0.1%_30_3	1.29	1.032
0.3%_30_3	1.28	1.024
0.5%_30_3	1.3	1.04
0.1%_40_2	1.3	1.04
0.3%_40_2	1.31	1.048
0.5%_40_2	1.32	1.056
0.1%_40_3	1.3	1.04
0.3%_40_3	1.28	1.024
0.5%_40_3	1.3	1.04

Table B2 Thickness of EVA-g-PLA specimens in tensile testing

Sample	Thickness (mm)	S.D.
Modified EVA	0.29	0.03
Pure PLA	0.35	0.05
0.1%_30_2	0.22	0.01
0.3%_30_2	0.25	0.01
0.5%_30_2	0.23	0.01
0.1%_30_3	0.23	0.01
0.3%_30_3	0.234	0.01
0.5%_30_3	0.27	0.01
0.1%_40_2	-	-
0.3%_40_2	0.24	0.03
0.5%_40_2	0.3	0.02
0.1%_40_3	0.27	0.06
0.3%_40_3	0.31	0.03
0.5%_40_3	0.23	0.01
0.1%_150_2	0.13	0.03
0.3%_150_2	0.2	0.03
0.5%_150_2	0.13	0.02
0.1%_150_3	0.2	0.02
0.3%_150_3	0.1	0.02
0.5%_150_3	-	-

ต้นฉบับ หน้าขาดหาย